Cross-Species BAC Transgenesis Reveals Long-Range Regulation Drives Variation in Brain Oxytocin Receptor Expression and Social Behaviors

Mina Tsukamoto [1], Luis AE Nagai[2], Kiyoshi Inoue[3], Lenin C. Kandasamy [1], Maria F. Pires[1], Minsoo Shin[1], Yutaro Nagasawa[1], Tsetsegee Sambuu[1], Kenta Nakai[4], Shigeyoshi Itohara[5], Larry J Young[3,6,7#], Qi Zhang[1,5,6,8*]

[1]Laboratory for Social Neural Networks, Faculty of Human Sciences, University of Tsukuba, Japan305-8577; [2] Laboratory of Computational Genomics, Institute for Quantitative Biosciences, The University of Tokyo, Japan113-0032; [3]Center for Translational Social Neuroscience, Emory National Primate Research Center, Emory University, USA30329; [4]Laboratory of Functional Analysis in silico, Human Genome Center, The University of Tokyo, Tokyo, Japan108-8639; [5]Laboratory for Behavioral Genetics, CBS, RIKEN, Japan351-0198; [6]Center for Social Neural Networks, Faculty of Human Sciences, University of Tsukuba, Japan305-8577; [7]Department of Psychiatry and Behavioral Science, Emory University, USA30329; [8] Institute for Glyco-core Research, Tokai National Higher Education and Research System, Gifu University, Japan501-1193

[#]Deceased in March, 2024. **We dedicate this work to the memory of Dr. Larry J. Young, whose encouragement and unwavering support helped our team persevere through challenges.**

*Correspondence: zhang.qi.b3@f.gifu-u.ac.jp or zhangqi@human.tsukuba.ac.jp or qi.zhang@a.riken.jp

Classification: Biological Science: Neuroscience

Keywords: oxytocin system, behavioral evolution, bacterial artificial chromosome (BAC), brain, mammary gland, partner preference, maternal care, topologically associating domain (TAD), evolvability.

The PDF file includes:

Main Text

Figures 1 to 7

Supplementary Figures 1to 3, supplementary Tables 1

Abstract

Although oxytocin (OXT) exhibits a highly conserved neuroanatomical pattern among vertebrates, the distribution of OXT receptor (OXTR) in brain varies considerably across species and is associated with species-typical social behavior. To investigate the genomic basis of the phylogenetic plasticity in brain *Oxtr* expression and its social behavioral consequences, we generated transgenic mice carrying a bacteria artificial chromosome (BAC) harboring the entire prairie vole *Oxtr* locus and flanking intergenic regulatory regions. We established eight independent "volized" mouse lines expressing prairie vole *Oxtr* (pv*Oxtr*). Strikingly, despite conserved *Oxtr* expression in mammary gland of all transgenic mouse lines, each line displayed a unique pattern of brain expression distinct from both mice and prairie voles. Together with topologically associating domain (TAD) structure analysis with mouse genome, our findings suggest that unlike *Oxt*, *Oxtr* expression patterns in brain, involve contributions of distal regulatory elements beyond the BAC insert. In contrast, *Oxtr* expression in peripheral tissues appears resistant to such distal influences. Moreover, the "volized" mouse lines with different brain *Oxtr* expression patterns showed differences in partner preference and maternal behaviors, providing direct functional evidence that variation in brain *Oxtr* expression can drive differences in social behaviors. We propose that brain *Oxtr* expression is transcriptionally

53 sensitive to long-range interactions with distal genomic elements, rendering it more
54 susceptible to diverse regulatory influences. This supports a model in which regulatory
55 flexibility facilitates the evolutionary diversification of social behavior, while maintaining
56 essential peripheral *Oxtr* expression.

57 **Highlights**

58 Unlike essential physiological phenomenon including feeding, sex, parturition and
59 lactation, which are conserved across mammalian species, there is extraordinary diversity
60 of social behaviors between and within species. Comparative studies across species suggest
61 that variation in brain oxytocin receptor expression may mediate diversity in social
62 behavior. Subtle variations in human oxytocin receptor sequence have been related to
63 psychiatric phenotypes. Our studies suggest that the oxytocin receptor gene is
64 hypersensitive to long-distance sequence variation, as revealed by differential expression
65 patterns when the BAC transgene was inserted at different genomic sites, leading to
66 variability in brain expression and social behavior. This research provides new insights into
67 the evolvability of genes producing diversity in social behaviors, which allows efficient
68 adaptation of animals to variable environment. Furthermore, our cross-species study
69 demonstrates that diversity in brain OXTR expression patterns leads to variation in mouse

social behaviors. The "volized" *Oxtr* mouse lines generated here present a valuable resource for further exploring OXTR expression regulation and neural circuits/networks mediating social behavioral variability.

Introduction

Brain oxytocin receptors (OXTR) regulate a wide range of social behaviors including social recognition, maternal care, social bonding, empathy related behaviors, and aggression (Froemke & Young, 2021; Jurek & Neumann, 2018; Rigney, de Vries, Petrulis, & Young, 2022). In contrast to sex steroid receptors, which have highly conserved brain expression patterns across species, OXTR shows remarkable inter- and intra-species variation in brain distribution (Froemke & Young, 2021; Larry J. Young & Zhang, 2021). For example, monogamous prairie voles have a brain OXTR distribution in cortex, striatum and amygdala that is significantly distinct from promiscuous montane voles and laboratory rats and mice(Larry J. Young & Zhang, 2021). Furthermore, there is robust individual variation in brain OXTR expression among prairie voles that is associated with single nucleotide polymorphisms (SNPs) in the OXTR locus (*Oxtr*), and this variation predicts pair bonding behavior and resilience to early life social neglect (Ahern, Olsen, Tudino, & Beery, 2021; Barrett, Arambula, & Young, 2015; King, Walum,

88 Inoue, Eyrich, & Young, 2016; Ross et al., 2009). Different species of primates also differ
89 in brain OXTR distribution (Rogers Flattery et al., 2022), and SNPs in the human OXTR
90 have been linked to variation in social function (Skuse et al., 2014; Theofanopoulou,
91 Andirkó, Boeckx, & Jarvis, 2022). Thus, variation in OXTR distribution in brain likely
92 constitutes a mechanism for the emergence of diverse social traits, potentially including
93 psychiatric endophenotypes.

94 The evolution of gene expression patterns could be mediated by *cis* (via linked
95 polymorphisms) or *trans* (through diffusible products of distal genes, e.g., transcription
96 factors) changes, as a result of adaptation to the environment (Mack, Campbell, &
97 Nachman, 2016; Osada, Miyagi, & Takahashi, 2017; Shi et al., 2012). *Cis*-regulatory
98 differences are more commonly responsible for adaptive evolution and interspecific
99 divergence (Signor & Nuzhdin, 2018). To explore the transcriptional mechanisms giving
100 rise to species-specific *Oxtr* expression and social behavior, we created transgenic mice
101 using a prairie vole *Oxtr* (pv*Oxtr*) bacterial artificial chromosome (BAC). The BAC
102 construct covers the full coding sequence, introns and the entire intergenic region of the
103 pv*Oxtr* with its neighboring genes. We expected that our BAC construct accommodates
104 all the critical regulatory sequences responsible for species- and tissue-specific
105 expression, so that pv*Oxtr* transgenic mice would express brain pv*Oxtr* in a prairie vole-

like pattern, largely independent of integration sites. Then we would examine if our transgenic mouse could develop social behaviors similar to that of prairie vole.

We generated eight pv*Oxtr* mouse lines with successful germline transmission. Each line, defined by a distinct BAC integration site, exhibited a unique brain-specific expression pattern of *Oxtr*, distinct from both wildtype mice and prairie voles. Notably, *Oxtr* expression in the mammary gland was conserved across all lines. This suggests that brain, but not mammary gland, expression of *Oxtr* is shaped by distal regulatory elements beyond the BAC insert. These findings imply that evolution has placed brain *Oxtr* expression under more complex regulatory control, likely to accommodate the diversification of social behaviors, whereas mammary gland expression is maintained by simpler mechanisms supporting conserved lactation functions. Furthermore, behavioral assays revealed line-specific differences in partner preference and maternal behaviors.

The 3D architecture of the genome, segregated into TADs demarcated by CCCTC-binding factor (CTCF), crucially influences gene expression. Through the loop extrusion model, CTCF enables interactions between distant regulatory elements, facilitating precise gene regulation, which ultimately shapes an organism's phenotype and behavior(Wendt et al., 2008). Hi-C data provide a genome-wide view of chromosome conformation in multiple layers, such as compartments, TADs, and loops(Gibcus &

Dekker, 2013; Lieberman-Aiden et al., 2009). Our TAD analysis with Hi-C database showed a clear difference exists between the 3D structures of *Oxt* and *Oxtr* gene, and a clear difference exists between the 3D structures of brain tissue *Oxtr* and peripheral tissue *Oxtr*, suggesting that Oxtr expression patterns in brain depends on contributions from very distal sequences. These results provide important clues to understand the genetic mechanism underlying species differences in brain gene expression.

Together, our data demonstrate that transcriptional redistribution of brain *Oxtr* can drive variation in social and parental behaviors—variation that natural selection could act upon in specific ecological contexts. Our results also offer insights into the genetic mechanisms underlying species-specific brain gene expression.

141 # Results

142 **Creation of the pv*Oxtr-P2A-Cre* BAC transgenic mice**

143 BAC vectors can accommodate dispersed cis-regulatory elements across large regions of
144 genome. Transgene expression from BAC constructs are generally resistant to insertion
145 position effects (Suster, Abe, Schouw, & Kawakami, 2011) due to both the large spans of
146 insulating genetic material which protect the transgene cassette from the influence of the
147 chromosomal environment, and through the inclusion of necessary regulatory elements
148 such as enhancers, silencers, locus control regions, and matrix attachment regions (Beil,
149 Fairbairn, Pelczar, & Buch, 2012; Bian & Belmont, 2010). Large-scale screening of CNS
150 gene expression in BAC transgenic mice by the GENSAT (Gene Expression Nervous
151 System Atlas) Project found that more than 85% of BACs express reproducibly in
152 multiple independent transgenic lines and reporter gene expression faithfully recapitulates
153 endogenous gene expression patterns (Gerfen, Paletzki, & Heintz, 2013; Heintz, 2004;
154 Schmidt, Kus, Gong, & Heintz, 2013). Indeed, reproducible expression from mouse BAC
155 vectors has been achieved for more than 500 genes (Gerfen et al., 2013; Heintz, 2004;
156 Schmidt et al., 2013). Few that don't express reproducibly are influenced by variation in
157 BAC copy number and insertion sites (S. Gong et al., 2007). BAC engineering has also
158 been used to mediate cross-species transgene expression. A large number of mouse

159 models of human dominant neurodegenerative disorders have been created using human
160 BAC transgene approaches. These model mice successfully express human transgenes in
161 human-like patterns and recapitulate disease-like phenotypes (Crook & Housman, 2011;
162 Ferrante, 2009; Shenoy et al., 2022; Taguchi et al., 2019; Yang & Lu, 2008). Previously
163 we constructed *Pkcd-BAC-Cre* transgenic mice and obtained independent lines with
164 reproducible expression patterns as well (Zhang et al., 2016)(Supplementary Fig.1).We
165 therefore decided to use BAC approaches to create "volized" *Oxtr* mouse lines.
166 To create pv*Oxtr-P2A-Cre* BAC transgenic mouse line, the prairie vole BAC clone we
167 used includes the entire pv*Oxtr* locus (the coding sequence and all the introns) with the
168 full intergenic sequence upstream (150kb) and downstream of the pv*Oxtr* coding region
169 (9kb) (Fig.1 B). The BAC clone contains a portion of *Rad18,* minus the first 11 exons*,*
170 located upstream of pv*Oxtr,* and *Cav3*, minus the first exon including the start codon,
171 downstream of pv*Oxtr.* Therefore, there will be no interference of these two flanking
172 transgenes on behavior analysis*,* and the proximal topological structure around pv*Oxtr*
173 locus is preserved to the maximum extent. A P2A-NLS-Cre cassette was inserted in-
174 frame just before the *Oxtr* stop codon to ensure co-expression of *Cre* and *Oxtr* (Fig.1 C).
175 Transgenic mice were generated by pronuclear injection using C57BL/6J zygotes. Proper
176 integration of the reporter into the BAC clone was confirmed using gene specific PCR

177 assays and sequencing (Fig.1 C, D and data not shown). We obtained 11 founder mice
178 carrying the transgenes, which was verified by PCR with multiple primer sets (Fig.1 C,
179 E). One founder line was sterile, and two founder lines did not show germ-line
180 transmission. Eight founder lines successfully produced offspring and stably transmitted
181 the transgene to at least 3 generations. We named these lines "Koi", meaning "love" in
182 Japanese.

183

184 **Each Koi line showed a unique expression pattern of transgene in brain, yet**
185 **conserved expression in mammary gland.**

186 We systemically evaluated 8 Koi lines by crossing them with ROSA-26-NLS-*LacZ* mice,
187 a Cre reporter mouse line expressing nuclear-localized beta-galactosidase (Kandasamy et
188 al., 2021; Zhang et al., 2016). Since Lac-Z is only expressed in the nucleus of double
189 positive (CRE+, LacZ+) cells, but not in the neuronal processes, we could easily assess
190 the expression pattern of our transgene. We found that each Koi founder line displayed a
191 unique pattern of expression in brain distinct from that of wildtype mice or prairie voles
192 (Fig.2 A-O, and supplementary Fig.2). Almost all Koi lines showed transgene expression
193 in olfactory bulb, lateral septum (Fig.2 F-I and Supplementary Fig.2 B,E,H,K) and
194 ventromedial nucleus of the hypothalamus (Fig.2 K-N and Supplementary Fig.2 C,F,I,L),

195 though with different intensities, suggesting that these regions constitute a stable core
196 *Oxtr* expression network, as these regions also express OXTR in mice and voles (Inoue,
197 Ford, Horie, & Young, 2022; Newmaster et al., 2020). Several Koi lines expressed the
198 transgene in some brain regions specific for vole *Oxtr* expression, including nucleus
199 accumbens (NAc) (Fig.2 A,B,D and Supplementary Fig.2 A,G,J), prefrontal cortex (PFC)
200 (Fig.2 A,B,C and Supplementary Fig.2 J), lateral amygdala (Fig.2 K,L,M and
201 Supplementary Fig.2 C,I,L) and deep layers of cingulate cortex (Fig.2A,B,C and
202 Supplementary Fig.2 C,L), which suggested that cis regulatory elements in the BAC are
203 capable of mediating the expression of *Oxtr* in the reward and reinforcement circuitry of
204 brain, albeit depending on the sequence/structure of distal sequences >150 kb upstream
205 and >21 kb downstream of the transcription start site. None of the Koi lines exactly
206 "mirrored" the vole-specific expression patten. Six of the Koi lines expressed the
207 transgene in broad areas of thalamus (Fig.2 K,L,N and Supplementary Fig.2 C,I,L),
208 reminiscent of the strong expression of V1a vasopressin receptor (*Avpr1a*) in the
209 thalamus (Larry J. Young & Zhang, 2021). Intriguingly, the expression of OXTR in
210 mammary glands showed similar pattern among all the Koi lines and *mouseOxtr(mOxtr)-*
211 *Ires-Cre* knock-in line (Fig.2 P-T and Supplementary Fig.3).

212 Transgenes that are introduced by pronuclear injection typically integrate into a single
213 site of the genome as tandem concatemers (Smirnov et al., 2019). BAC copy number
214 variation and different insertional loci can lead to distinct patterns of ectopic expression,
215 and increased BAC transgene copy numbers often correlate with increased BAC gene
216 expression (S. Gong et al., 2007). We then examined the relationship between transgene
217 copy number and LacZ signal using quantitative genomic PCR (Chandler et al., 2007). As
218 expected, the copy number of WT, heterozygous and homozygous *mOxtr-Ires-Cre* knock-
219 in mice was 0, 1 and 2 respectively (Figure.2 Z). The copy number of transgene in Koi
220 lines are: Koi-1 (12), Koi-2 (2), Koi-3 (2), Koi-4 (1), Koi-5 (2), Koi-6 (4), Koi-7 (9), Koi-
221 8 (3). Koi-6 and Koi-7 showed the most limited expression of reporter gene, though the
222 copy number of transgene were 4 and 9 respectively. Koi-4 showed strong expression of
223 reporter gene in NAc, septum and thalamus, though there was only 1 copy of transgene.
224 Therefore, integration site rather than copy number is the reason of the variant BAC
225 transgene expression patterns across our Koi lines.

226

227 **Adult brain OXTR binding patterns differ across Koi lines**

228 To detect the distribution of OXTR protein in adult Koi lines without the interference of
229 endogenous mouse OXTR (mOXTR) signal, Koi lines were crossed with *mOxtr*$^{-/-}$ line

230 twice sequentially to produce Koi: m*Oxtr*$^{-/-}$ mice, and pvOXTR binding was detected
231 using receptor autoradiography. We focused on analyzing 4 lines: Koi-1: m*Oxtr*$^{-/-}$, Koi-2:
232 m*Oxtr*$^{-/-}$, Koi-3: m*Oxtr*$^{-/-}$ and Koi-4: m*Oxtr*$^{-/-}$ based on the strong expression of reporter
233 gene in behaviorally relevant neuronal populations. Autoradiography demonstrated
234 functional pvOXTR in brain resembling to some extent Cre-induced reporter gene
235 expression (Fig.3). Brain OXTR binding of Koi-3: m*Oxtr*$^{-/-}$ was consistent with Lac-Z
236 expression in the reporter line (Fig.2 C, H, M and Figure.3 C, H, M). Interestingly, the
237 OXTR binding in PFC of Koi-3: m*Oxtr*$^{-/-}$ was similar to that of prairie vole (Figure.3 C).
238 In contrast, Koi-4: m*Oxtr*$^{-/-}$ showed low OXTR binding in NAc when compared with the
239 high Lac-Z staining (Fig.2 D and Figure.3 D). Koi-2: m*Oxtr*$^{-/-}$, the line which displayed
240 the expression of reporter genes in the broadest regions, did not show strong signal in
241 autoradiography. It is interesting that Layer IV of cortex in Koi-4: m*Oxtr*$^{-/-}$ showed
242 strong OXTR binding (Figure.3 I and N), which is highly likely to originate from the
243 axon projections from the thalamus (Fig.2 N), as was previously reported for NAc
244 projections in voles (Inoue et al., 2022). Consistent with Lac-Z expression, we do not see
245 a clear relationship between OXTR binding and transgene copy number. For example,
246 Koi-1: m*Oxtr*$^{-/-}$ showed rather low OXTR signal (Fig.3 A, F, K) with the highest copy

247 number, while Koi-4: m*Oxtr*$^{-/-}$ showed very strong OXTR signal at lateral septum and
248 thalamus (Fig.3 I, N), with the lowest copy number.

249 *Oxtr* mRNA level in Koi-3: m*Oxtr*$^{-/-}$ and Koi-4: m*Oxtr*$^{-/-}$ was further investigated with
250 Fluorescent RNAscope *in situ* hybridization (Fig.4). Consistent with Lac-Z expression in
251 the reporter line, Koi-3: m*Oxtr*$^{-/-}$ showed strong signal in PFC and Ctx (Fig.4 A, C), while
252 Koi-4: m*Oxtr*$^{-/-}$ showed prominent signal in NAc and Thalamus (Fig.4 B, D). qRT-PCR
253 analysis further revealed that adult Koi-4: m*Oxtr*$^{-/-}$ mice had the highest Oxtr mRNA
254 signal in the ventral striatum, several fold higher than WT, consistent with the Lac-Z
255 staining in the reporter line (Fig.5 A, B). The discrepancy of OXTR signal in NAc of
256 Koi-4: m*Oxtr*$^{-/-}$ between autoradiography and Lac-Z staining /RNAscope/qRT-PCR may,
257 therefore, be due to the translational regulation or differences in the sensitivity of the
258 detecting methods.

259 Although none of our Koi lines mirrored the endogenous OXTR expression in prairie
260 voles, we confirmed strong expression of pv*Oxtr* in olfactory bulb of Koi-1line, PFC and
261 amygdala of Koi-3line, striatum and thalamus of Koi-4 lines, and the broad expression of
262 pv*Oxtr* in Koi-2 line. As OXTR signaling in some of these regions are similar to that in
263 voles, albeit in separate lines, and postulated to be involved in vole social behavior (H.

264 Walum & L. J. Young, 2018), we used these lines to address the question of whether
265 variation in *Oxtr* transcription in brain can lead to variation in social behaviors.
266

267 **Different Koi lines showed diverse behaviors in a Partner Preference Test**

268 The partner preference test is widely used as a laboratory proxy for pair bonding in
269 prairie voles. In a pilot study, we found that Kio-4 female mice on a m*Oxt*$^{+/+}$ background
270 showed a preference for their mate relative to a novel male. We then focused on the
271 females of 4 lines (Koi-1, 2, 3, 4) based on transgene expression in PFC, BLA or NAc.
272 Again, we bred the Koi lines with *mOxtr*$^{-/-}$ mice (both on C57/B6 background) to
273 generate Koi: m*Oxtr*$^{-/-}$ offspring expressing only pv*Oxtr*. Partner preference tests (PPT)
274 were performed in ovariectomized females after 21 days of cohabitation with 3 mating
275 bouts elicited by estrogen and progesterone injections on days 2, 9 and 16. We divided
276 our analysis into 3 phases (Fig.6 A, B). In the habituation phase, the experimental subject
277 was habituated to the chamber for 5 minutes with both pen-boxes empty. In the
278 recognition phase, the partner stimulus animal was restricted in one pen-box, and a novel
279 "stranger" male was restricted in another pen-box, and the experimental female was
280 allowed to explore the arena for 10 minutes to test social novelty preference. In the
281 preference phase, the positions of the partner stimulus animal and the "stranger" stimulus

282 animal were switched to avoid position bias, and the female was allowed to explore the
283 chamber for an additional 20 minutes.

284 Mixed ANOVA was conducted to examine the effect of genotype and the stimulus box on
285 the area stay time during all the phases. In the habituation phase (Fig.6 C), there was no
286 statistically significant interaction between the effects of genotype and position of empty
287 pen-box on stay time, $F(4, 60) = 0.69$, $p = 0.6$. There was no difference in position preference
288 for all the groups, $F(1,60) = 0.03$, $p = 0.87$. In the recognition phase (Fig.6 D), there was a
289 main effect of stimulus animal (i.e., partner or stranger) on stay time, the time staying in
290 close proximity to the partner was significantly shorter than the time stay with stranger
291 animal ($F(1,60) = 15.38$, $p = 0.0003$). There was a main effect of genotype on social stay
292 time, $F(4,60) = 2.62$, $p = 0.04$, and a significant interaction between the effects of genotype
293 and stimulus animal on area stay time, $F(4, 60) = 2.61$, $p = 0.04$. Bonferroni adjusted
294 pairwise comparisons were applied to analyze the simple main effects. Koi-4: m*Oxtr*$^{-/-}$ and
295 WT mice spent significantly longer time in "stranger" area than in "partner" area ($p = 0.0001$
296 for Koi-4: m*Oxtr*$^{-/-}$; $p = 0.028$ for WT), demonstrating a typical novelty preference. There
297 was no significant difference between the stay time with "stranger" and "partner" for Koi-
298 1: m*Oxtr*$^{-/-}$ ($p = 0.96$), Koi-2: m*Oxtr*$^{-/-}$ ($p = 0.49$) and Koi-3: m*Oxtr*$^{-/-}$ ($p = 0.09$) mice. In the
299 preference phase (Fig.6 E), conducted after both stimulus mice were presumably familiar

following the initial 10 min recognition phase, there was no main effect of stimulus animal on stay time, F (1,60) =0.04, p=0.84. There was no main effect of genotype on stay time either, F (4,60) =1.36, p=0.26. There was a statistically significant interaction between the effects of genotype and stimulus animal on area stay time, F (4, 60) = 4.64, p=0.003. Bonferroni adjusted pairwise comparisons revealed that Koi-2: m*Oxtr*$^{-/-}$ mice spent significantly longer time in "stranger" area than in "partner" area (p=0.024). In contrast, Koi-4: m*Oxtr*$^{-/-}$ mice spent significantly longer time in "partner" area than in "stranger" area (p=0.002). There was no significant difference between the stay time with "stranger" and "partner" for WT (p=0.99), Koi-1: m*Oxtr*$^{-/-}$ p=0.16) or Koi-3: m*Oxtr*$^{-/-}$ (p=0.45) mice.

Different Koi lines showed diverse behaviors in Pup Retrieval Test

Based on the abundant pvOXTR of Koi-3and Koi-4 in reward-related brain regions (Fig.3 C,D,H,I,M,N), and the role of OXTR in mediated maternal care in mice and voles (Carcea et al., 2021; Marlin, Mitre, D'Amour J, Chao, & Froemke, 2015; Olazábal & Young, 2006), we further tested the parental behaviors of these two lines in virgins (Fig.6 F, G). Mixed ANOVA was conducted to examine the effect of genotype and pup number (1-3) on the latency of pup retrieval. Mauchly's test showed that the sphericity was violated. Therefore, the Greenhouse-Geisser correction was used for the repeated

measures ANOVA. There was a significant main effect of genotype on latency to retrieve, F (2,48) =29.58, p<0.0001. Koi-4: m*Oxtr*$^{-/-}$ took a significantly longer time to retrieve all the pups than WT and Koi-3: m*Oxtr*$^{-/-}$ (p<0.0001 for both). There was also a significant interaction between the effects of genotype and retrieved pup number on the retrieval latency, F (2.40, 57.49) = 4.45, p =0.011. Post Hoc multiple comparisons with Bonferroni correction revealed that Koi-4: m*Oxtr*$^{-/-}$ took a significantly longer time to accomplish the 1st retrieval (p=0.0003 and p=0.0005), the 2nd retrieval (p<0.0001), and the 3rd retrieval (p<0.0001) when compare to WT and Koi-3: m*Oxtr*$^{-/-}$. And Koi-3: m*Oxtr*$^{-/-}$ took a significantly shorter time to accomplish the 1st retrieval (p=0.01), the 2nd retrieval (p=0.006), and the 3rd retrieval (p=0.003) when compare to WT.

Crouching time was analyzed as well (Fig.6 F, H). There was a statistically significant difference between groups as determined by one-way ANOVA (F (2,48) = 27.56, p <0.0001). A Bonferroni post hoc test revealed that the crouching time of Koi-3: m*Oxtr*$^{-/-}$ was statistically significantly longer than WT (p=0.008) and Koi-4: m*Oxtr*$^{-/-}$ (p<0.0001). Additionally, the crouching time of Koi-4: m*Oxtr*$^{-/-}$ was statistically significantly shorter than WT (p=0.001). Therefore, two Koi lines with different OXTR expression pattern demonstrated quantitative differences in parental behavior tests.

The TAD structure of brain *Oxtr* is markedly distinct from that of both *Oxt* and peripheral *Oxtr*.

The divergent brain expression patterns across our Koi lines suggest that distal elements external to our BAC cassette contribute to the variation in *Oxtr* expression. TADs represent a key feature of hierarchical genome organization comprising regions of high chromatin inter-connectivity, and TAD formation appears to be linked to transcription regulation (Beagan & Phillips-Cremins, 2020; Dekker, Rippe, Dekker, & Kleckner, 2002; Dixon et al., 2012; Rajderkar et al., 2023). TADs are generally conserved within the same tissue type across different species. We therefore utilized publicly available 3D chromatin datasets from mouse (Extended data Table7-1) and analyzed the TAD structure of *Oxtr* and *Oxt*, both in brain related tissues/cells and peripheral tissues/cells. We discovered that *Oxtr* is consistently located at the boundary region of TAD structures across several tissues and cell lines (Fig.7 A). Specifically, only in brain related samples (whole brain tissue, neural progenitor cells, and cortex tissue), *Oxtr* is situated at the boundary of a large inter-TAD interaction between two neighboring TADs (Fig.7 A). In contrast, the oxytocin peptide gene, *Oxt*, which is expressed in a highly conserved brain pattern across vertebrates, lacks organized TAD structures (Fig.7 B). These findings demonstrate that the TAD landscape differ dramatically between *Oxtr* and *Oxt*, and highlight that the 3D

genomic architecture surrounding the *Oxtr* gene varies between brain tissues/cells and peripheral tissue/cells. There exists clear long-distance interaction in brain *Oxtr* gene TAD structure. The presence of extensive long-distance chromatin interactions around *Oxtr* in brain tissues may at least partially explain why its expression is hypersensitive to distal regulatory sequences beyond the range of a BAC construct. Moreover, such large inter-TAD interactions likely expose *Oxtr* regulation to a broader set of cis- and trans-acting influences, rendering brain *Oxtr* expression inherently more variable across individuals and species.

Discussion

Diversity of *Oxtr* expression patterns causes diversity of social behaviors

The diverse OXTR expression of our Koi lines is reminiscent of the diverse OXTR expression across different species. The unique expression pattern of *Oxtr* in monogamous prairie vole was mainly observed in PFC, NAc and BLA. We obtained expression in all of these specific regions, but in 3 separate lines. These Koi lines with distinct brain OXTR expression pattern provided an opportunity to test the effect of variation of OXTR expression on diverse social behaviors.

371 It is intriguing that Koi-4 line showed preference to their mating partners but not
372 strangers, which is a behavior specific in prairie voles but not in mice. Multiple studies
373 suggested that NAc and PFC play important roles in mediating partner preference
374 behavior in prairie voles (Amadei et al., 2017; Hasse Walum & Larry J. Young, 2018).
375 Consistently, the Koi-4 line showed robust transgene expression in these brain regions.
376 Notably Koi-4 line also demonstrated strong *Oxtr* expression in the entire thalamus
377 region, which reminds us the distribution of *Avpr1a* (Phelps & Young, 2003). Given the
378 fact that OXTR and AVPR1A genes were derived from a duplication of a single ancestral
379 gene (Grinevich, Knobloch-Bollmann, Eliava, Busnelli, & Chini, 2016), it is not
380 surprising that the similar expression regulation machinery exists. Recent studies indeed
381 revealed the critical functions of different thalamic nuclei in social memory and cognition
382 (Chen et al., 2024; Kappel et al., 2022; Rangel, Baldo, & Canteras, 2018; Wolff & Vann,
383 2019). Partner preference formation and maintenance needs to recruit multi- and cross-
384 modality sensation, social recognition and social memory, selective attention, arousal,
385 and reward systems. We propose a model that the sufficient upregulation of the OXTR
386 expression in one or multiple of these systems can tune the network and boost partner
387 preference behavior. In addition, the maternal behavior in Koi-3 and Koi-4 lines was
388 enhanced and reduced, respectively. This result suggested that OXTR signaling facilitates

social partner preference and maternal care by coordinating activity across different neural networks. A main conclusion of our study is that simply by redistributing OXTR binding in space, variation in social preference and parental behaviors emerged, which conceivably could impart advantageous behaviors that natural selection could act upon and amplify. Future study will determine how the variation in OXTR distribution in our Koi lines affects neural circuits mediating social behaviors.

A potential genetic mechanism contributing to diversity of brain OXTR expression

The sex steroid and oxytocin systems play important roles in modulating reproductive and related social behaviors in vertebrates. Sexual behavior, e.g., the motivation to mate and motor patterns, is highly conserved across vertebrate species. By contrast, social behaviors, e.g., sociality, mating strategy (monogamy vs polygamy), parental and alloparental behaviors are more nuanced and can vary dramatically across species in the same genus or even between individuals of a single species. It is interesting, therefore, that the distribution of steroid receptors is quite conserved among species (L. J. Young & Crews, 1995), while that of the OXTR is extremely diverse across and even within species (Froemke & Young, 2021; Larry J. Young & Zhang, 2021). It is even more interesting that although the distribution of OXTR is diverse, its ligand, oxytocin, is

407 expressed in a highly conserved neuroanatomical pattern in vertebrates (Ross & Young,
408 2009). Previous work showed that three independent rat lines with puffer fish oxytocin
409 BAC transgene (containing 16 kb of 5' flanking regulatory sequence) expressed the *Fugu*
410 oxytocin transcript specifically in oxytocin neurons in rat (Venkatesh, Si-Hoe, Murphy, &
411 Brenner, 1997). Moreover, a similar transgenic experiment transferring approximately 5
412 kb of the *Fugu* oxytocin already resulted in a faithful expression of the fish genes in
413 mouse oxytocin neurons (Gilligan, Brenner, & Venkatesh, 2003). These studies suggest
414 there is a remarkably conserved transcriptional regulatory machinery across species, even
415 between the *Fugu* and rodent oxytocin genes, despite being separated by 400 million
416 years of evolution.
417 The GENSAT (Gene Expression Nervous System Atlas) Project demonstrated that most
418 BAC transgenes reliably recapitulate endogenous expression across independent lines,
419 provided that extensive flanking intergenic regions are included (Gerfen et al., 2013; S.
420 Gong et al., 2007; Shiaoching Gong et al., 2003; Heintz, 2004; Schmidt et al., 2013). Our
421 pv*Oxtr* clone contained the entire locus with full upstream and downstream intergenic
422 sequences, yet the transgenic lines we generated displayed strikingly divergent brain
423 expression patterns. These differences were not explained by transgene copy number, but
424 instead reflected strong insertion-site effects. This paradox contrasts with the general

425 reproducibility of BAC transgenics and echoes the observation that virtually every rodent
426 or primate species has a unique distribution of OXTR binding in the brain.
427 The 3D genomic structure analysis showed that the *Oxtr* loci sit within large TAD
428 structures, increasing its exposure to distal regulatory elements through an expanded
429 interaction landscape, whereas *Oxt* lacks organized TAD structures. This difference
430 might explain why short promoter sequences suffice for conserved *Oxt* expression across
431 species, while even a large BAC is insufficient for precise, reproducible transcription
432 regulation of *Oxtr*. The large TAD and extensive long-range interactions render *Oxtr*
433 especially sensitive to chromosomal context, accounting for the position effects we
434 observed.
435 It is also noteworthy that pv*Oxtr* expression in mammary gland (which is responsible for
436 essential lactation in mammals) was conserved across all Koi lines, indicating that the
437 essential cis-regulatory elements for peripheral expression are captured within the BAC
438 and are resistant to position effects. This conclusion is consistent with the chromatin
439 architecture we observed: the chromatin landscape differs considerably between brain-
440 related tissues and peripheral tissues. There exists an obvious increase of long-distance
441 interactions between neighboring TADs, forming a larger TAD structure in brain-related
442 tissues but not peripheral tissues. Moreover, critical peripheral regulatory sequences may

be clustered proximally around the locus, so that they fall entirely within the BAC. By comparison, in brain tissues, regulatory elements are dispersed across a much broader genomic interval, extending beyond the BAC. Together, the larger interaction landscape and distributed regulatory architecture in brain tissues likely explain why BAC constructs are sufficient for peripheral but not brain expression of *Oxtr*.

This is well aligned with broader principles of genome organization: subtle changes within 3D chromatin structure may result in substantial changes in local gene expression (Xiao, Hafner, & Boettiger, 2021). TADs also display increased SNPs and structure variations (SVs) density and higher recombination rate compared to inter-TAD regions(Beagan & Phillips-Cremins, 2020; Dekker et al., 2002; Dixon et al., 2012; Rajderkar et al., 2023). In fact, SNPs in the *Oxtr* intron explains 74% of the variance in striatal *Oxtr* expression and social attachment in prairie voles (King et al., 2016) and it is possible that these SNPs near *Oxtr* are linked to variations of long-range chromosomal interaction. Collectively, these evidences support the notion that brain *Oxtr* expression is hyper-sensitive to genetic variation.

Such an organization may endow *Oxtr* with enhanced evolvability. Oxytocin is a secreted neuromodulator that can diffuse along axons and through the extracellular space(Leng & Ludwig, 2008; Mitre et al., 2016; Parmaksiz & Kim, 2025). Its functional effects depend

critically on the precise localization of its receptors, as the spatial distribution of oxytocin receptors determines the neural circuits engaged and the behavioral outcomes elicited. By making brain expression more reliant on distal regulatory sequences, *Oxtr* becomes subject to a wider range of cis- and trans-acting influences, rendering its expression in the brain inherently more variable across individuals and species. This variability allows oxytocin signaling to recruit novel neural circuits and modulate diverse aspects of social behavior, thereby contributing to the evolutionary diversification of sociality. Future studies should aim to resolve the precise mechanisms underlying this variability—for example, by identifying which distal regulatory elements physically interact with *Oxtr* within brain-specific chromatin architectures.

Ideas and Speculation

In summary, our results revealed that region-specific expression of *Oxtr* in the brain requires long-distance interactions between proximal and distal cis-regulatory elements. In contrast, many other genes remained consistent across BAC-transgenic lines, indicating that proximal regulatory sequences within the BAC were sufficient to drive faithful expression in these tissues, and that this expression was resistant to positional effects.

Our findings support a broader hypothesis: genes vary in their regulatory robustness and evolutionary flexibility. We propose a framework dividing genes into two broad classes based on their transcriptional architecture—rigid and flexible genes. Rigid genes—perhaps comprising the majority of the genome—maintain core life-sustaining functions (e.g., metabolism, motor function, development, reproduction) and are typically regulated by compact proximal elements. Their expression is stable across species, and across individuals within a same species. For such genes, BAC constructs often recapitulate endogenous expression reliably—examples include CamKII, Protein Kinase C Delta(Pkcd), and other genes characterized in large-scale projects like GENSAT.

In contrast, a subset of genes are flexible genes—such as neuromodulatory receptors like *Oxtr* and potentially *Avpr1a* and *Drd4 (Dopamine receptor D4)*— possess inherently more fragile or flexible transcriptional regulation. Their expression is highly sensitive to multiple factors including the chromatin landscape and complex long-range regulatory interactions. We hypothesize that this regulatory sensitivity is not a flaw but an evolutionary feature—what we term transcriptional evolvability. Subtle genetic or epigenetic changes, such as SNPs, structural variants, or chromosomal rearrangements, may lead to variation in neuromodulator receptor expression, thereby altering the modulation of preexisting neural circuits. Such changes could unmask cryptic behavioral

phenotypes or give rise to novel social traits without requiring changes to core neural architecture. For example, caregiving circuits might evolve into pair bonding, empathy, or romantic attachment, while defensive or aggressive circuits might become recontextualized into behaviors like jealousy or mate guarding.

This model of transcriptional evolvability helps explain why *Oxtr* and *Avpr1a* expression varies so markedly across and within species, while their ligands (*Oxt* and *Avp*) remain stably expressed. The functional consequence of receptor variability is amplified by the secreted and diffusive nature of these neuromodulators: even small shifts in receptor localization can profoundly alter which neural circuits are engaged and which behaviors are modulated. It also raises the possibility that the capacity for behavioral innovation is, at least in part, encoded in the regulatory fragility of a small set of genes. Our model carries profound implications. It suggests that the evolution of complex social behavior is driven not only by neural circuitry or protein function, but by the regulatory architecture of a small set of flexible genes. These genes serve as behavioral tuning knobs—sensitive to the chromosomal environment, and capable of generating diverse phenotypes in response to evolutionary or environmental pressures. This model also offers insight into variability in human social phenotypes, including those observed in psychiatric conditions such as autism or social anxiety disorders, where subtle changes in receptor

515 gene regulation may lead to major phenotypic shifts. Further research into the regulatory
516 logic of *Oxtr, Avpr1a*, and similar genes may reveal a generalizable mechanism by which
517 genome structure enables behavioral diversity and adaptation across the animal kingdom.
518
519
520
521
522
523
524
525
526
527
528
529
530
531
532

533 ## Materials and Methods

534 ***pvOxtr-P2A-Cre* BAC vector construction**.

535 The vole BAC clone (GeneBank: DP001214.1) containing the *Oxtr* locus was obtained

536 from a prairie vole BAC library (CHORI-232) (Lisa A. McGraw et al., 2010; L. A.

537 McGraw, Davis, Thomas, Young, & Thomas, 2012). The NLS (nuclear localization

538 signal)-Cre-Frt-Amp-Frt cassette was obtained from Dr. Takuji Iwasato, and was slightly

539 modified to introduce a P2A sequence (Kim et al., 2011). The P2A sequence was

540 introduced using PCR with the following primers:

541 fw5'- ATGGGAAGCGGAGCTACTAACTTCAGCCTGCTGAAGCAGGCTGGAGA

542 CGTGGAGGAGAACCCTGGACCTCTCGAAACTGACAGGAGAACCACC-3';

543 rv5'-AGACTGGAGTCCGCATAGCCCCCCTCCCCCGCCCCAGGCGCGGTGGGCC

544 AGGCAGGTGGCTCACCTTGACCAAGTTGCTGAAGTTCCTATTCC-3'. The P2A sequence is

545 underlined. And the resulting amplified cassette had the P2A upstream of the NLS-Cre.

546 Then the P2A-NLS-Cre-Frt-Amp-Frt cassette was inserted in-frame right before the stop

547 codon of Oxtr in the BAC clone using the Red/ET Recombineering kit (Gene Bridges

548 GmbH, Heidelberg Germany) after adding homologous arms by PCR with the following

549 primers: fw5'-CACCTTCGTCCTGAGTCGCCGCAGCTCCAGCCAGAGGAGCTG

550 CTCTCAACCATCTTCAGCAATGGGAAGCGGAGCTACTAAC-3';

551 rv5'-GAGGAGAGGGATACACACCAATAGGCACCTTATACAACTCCACGCAC

552 GGCCACCAGGGGCAGACTGGAGTCCGCATAGCC-3'. The ampicillin selection marker was

553 deleted with the 706-Flpe-induced recombination method (Gene Bridges Heidelberg

554 Germany). A correctly modified BAC clone was verified by using PCR at both the 5' and

555 3' junctions of the targeted insertion with the following primer pair: fr5'-

556 GCCTTCATCATCGCCATGCTCTT-3'(p2) and rv5'-GATGGCTGAGTG ACTGGCATCT-3'(p8);

557 The construct was further verified by sequencing using the following 7 primers specific

558 either for BAC vector or the p2A-NLS-Cre fragment:

559 5'- CCTGCAGCCAACTGGAGCTTC-3'(p1); 5'- CTTCCTTGGGCGCATTGACGTC-3'(p5);

560 5'-TACCTGTTTTGCCGGGTCAG-3(p4)；5'-GCCTTCATCATCGCCATGCTCTT-3'(p2)；

561 5'-CTGACCCGGCAAAACAGGTA-3'(p7)； 5'-TCCGGTTATTCAACTTGCACCATGC-3'(p6);

562 5'-GATGGCTGAGTGACTGGCATCT-3'(p8).

563

564 **Animals.**

565 **pv*Oxtr-P2A-Cre* BAC transgenic mouse lines (Koi lines)**. pv*Oxtr-P2A-Cre* BAC vector

566 was digested with NotI for linearization and to remove the pTARBAC vector backbone.

567 The *Vole-Oxtr-P2A-Cre* BAC linearized fragment was purified using CL-4B sepharose

568 (Sigma-Aldrich), and injected into pronuclei of C57BL/6J zygotes. Mice carrying the
569 BAC transgene were identified and confirmed using PCR with 5 pairs of primers: fr5'-
570 TCGACCAGGTTCGTTCACTC-3'(p3) + p7; p2+ p6; p2 +p7; p4 +p8; p2+p8. 8 lines (Koi-1~Koi-
571 8) were confirmed with successful transgene inheritance. These lines were maintained on
572 a congenic C57BL/6J background by backcrossing with wildtype C57BL/6J for
573 assessments of BAC DNA copy numbers and initial transgene expression analysis.
574 The ***ROSA-26-NLS-LacZ* mouse** line (Zhang et al., 2016) was obtained from Itohara Lab
575 at RIKEN.
576 The ***mOxtr-Ires-Cre* knock-in** (Hidema et al., 2016) and ***mOxtr*$^{-/-}$ mutant** (Takayanagi et
577 al., 2005) lines were obtained from Dr. Katsuhiko Nishimori at Tohoku University, and
578 both were backcrossed with C57BL/6J for more than 10 generations. Each Koi line and
579 *mOxtr-Ires-Cre* knock-in mice were crossed with *ROSA-26-NLS-LacZ* mice to generate
580 Cre^{+}, LacZ^{+} double positive mice for further gene expression analysis. Female Koi mice
581 were crossed with male m*Oxtr*$^{-/-}$ to produce offspring with the genotype of pv*Oxtr-P2A-*
582 *Cre*(Koi): m*Oxtr*$^{+/-}$. These offspring were then bred to produce Koi: m*Oxtr*$^{-/-}$ mice
583 expressing pv*Oxtr* while lacking endogenous *mOxtr*, and these mice were used for
584 autoradiography, qRT-PCR and behavioral tests. All mice were generated using
585 continuously housed breeder pairs and P21 as the standard weaning date. All the animal

586 procedures were approved by University of Tsukuba Animal Care and Use Committee.
587 Mice were housed under constant temperature and light condition (12 h light and 12 h
588 dark cycle), and received food and water ad libitum.
589

590 **Determination of transgene copy number**

591 Custom Taqman® MGB probes were synthesized by oligoJp (Thermo Fisher, Japan) for
592 detecting the transgenic *Cre* and the mouse *Jun* gene (internal control). The following
593 primer pairs and probes were used: for the *Cre* assay, fr5'-
594 ATGACTGGGCACAACAGACAAT-3'; rv5'- CGCTGACAGCCGGAACAC-3'; probe:
595 5'-FAM- AAACATGCTTCATCGTCGGTC CGG-MGB-3'; for *Jun* assay, fr5'-
596 GAGTGCTAGCGGAGTCTTAACC-3'; rv5'-CTCCAGACGGCAGTGCTT-3'; probe:
597 5'-VIC-CTGAGCCCTCCTCCCC-MGB-3'. Real-time PCR was performed using an
598 Applied Biosystem7500. Transgene copy number was determined through absolute
599 quantification (standard curve method) following the protocol described in (Chandler et
600 al., 2007). Briefly, 2 microliters (20 ng) of genomic DNA samples or copy number
601 standards were analyzed in a 20μL reaction volume with two primer-probe sets (*Cre,*
602 *Jun*). The data from transgenic samples were then compared to a standard curve of
603 calibrator samples that are generated by diluting purified BAC DNA (linearized) over a

604 range of known concentrations into wild-type mouse genomic DNA. In addition, no-
605 template controls were included in each experiment. All reactions were performed in
606 triplicate.
607

608 **Histology**

609 Adult mice (3-4month old), 4 male and 4 female from each line/ generation were
610 analyzed for 3 generations. Mice were perfused intracardially with 4% formalin in 0.1M
611 sodium phosphate buffer. Brains were embedded in 2% agarose in 0.1M PB and cut into
612 100-m-thick sections with a Micro-slicer (Dosaka, Kyoto, Japan). Mammary glands were
613 isolated from virgin female mice (2month old), 2 mice/each line were analyzed. The brain
614 slices and whole mount mammary glands preparation were stained in X-gal solution (5
615 mM K3FeCN6, 5mMK4FeCN6,2mMMgCl2, 0.02% NP-40, 0.01% Na-deoxycholate, 1
616 mg/ml X-gal in 0.1M PB) at 37°C for 6 hours and then were stained with hematoxylin.
617 All experiments were done with positive and negative controls (Cre^+, $LacZ^-$) to monitor
618 the reliability of the X-gal staining. Images were caught by Nanozoomer 2.0-HT slide
619 scanner (Hamamatsu Photonics).
620

621 **Receptor Autoradiography**

622 OXTR autoradiography was performed as previously described (Inoue et al., 2022).
623 Briefly, freshly frozen brains were stored at -80˚C. Coronal sections were cut in a cryostat
624 and 20 µm sections were collected and then stored at -80˚C until use in autoradiography.
625 Brain sections were removed from -80˚C storage and air dried, and then fixed for two
626 minutes with 0.1% paraformaldehyde in PBS at room temperature, and rinsed twice in 50
627 mM Tris buffer, pH 7.4, to remove endogenous OT. They were then incubated in 50 pM
628 125I-OVTA (2200 Ci/mmol; PerkinElmer; Boston, MA), a selective, radiolabeled OXTR
629 ligand, for one hour. Unbound 125I-OVTA was then washed away with Tris-$MgCl_2$
630 buffer (50 mM Tris plus 2% MgCl2, pH 7.4) and sections were air dried. Sections were
631 exposed to BioMax MR film (Kodak; Rochester, New York) for five days. Digital images
632 were obtained with a light box and a Cannon camera (Cannon 6D MarkII, Japan). The
633 brightness and contrast of representative images were equally adjusted for all
634 autoradiography images within a panel using Adobe Photoshop.
635

636 **Fluorescent RNAscope *in situ* hybridization for *Oxtr* mRNA localization**

637 RNAscope Multiplex Fluorescent Reagent Kit v2 (Advanced Cell Diagnostics, Newark,
638 California; Cat. No. 323270) was used according to the manufacturer's instructions.
639 Adjacent sections to those utilized for I-125 OVTA receptor binding autoradiography

640 were used. Briefly, sections were thawed and fixed in 10% neutral buffered formalin for
641 15 minutes followed by treatment with hydrogen peroxide for 10 minutes and RNAscope
642 Protease IV for 30 minutes. Probes specific to prairie vole *Oxtr* mRNA (Cat. No. 500721)
643 were then applied and allowed to hybridize for two hours at 40 °C. After three
644 amplification steps, hybridized probes were labelled with horseradish peroxidase (HRP),
645 and TSA Vivid Dye 570 fluorophore. Sections were counterstained with DAPI for nuclei
646 labeling and coverslipped with ProLong Gold Antifade Mountant (ThermoFisher
647 Scientific; Waltham, Massachusetts). Negative controls were performed using a bacterial
648 dapB probe (Cat. No. 310043), which did not exhibit any nonspecific labeling.
649 Fluorescent RNAscope images were acquired using a Keyence BZ-X710 microscope.
650 Whole sections were captured with 10x objective lens in two channels (red and blue), and
651 images were stitched together using Keyence BZX Analyzer Software. Brightness and
652 contrast of the images were adjusted using Photoshop (Adobe; San Jose, California).
653

654 **Quantification of *Oxtr* mRNA expression by qRT-PCR**

655 Real-time quantitative polymerase chain reaction (RT-qPCR) using an Applied
656 Biosystems 7500 Real-Time PCR system was used to quantify *Oxtr* mRNA expression
657 levels in different brain regions of Koi lines. Total RNA of different brain regions was

658 isolated using the RNeasy extraction kit (Qiagen, Germantown, US), and cDNA was
659 synthesized after Deoxyribonuclease I (Invitrogen, Waltham, US) treatment by using
660 EvoScript Universal cDNA Master (Roche, Penzberg, Germany), and then quantitative
661 RT-PCR was performed with FastStart Universal SYBR Green Master (Roche, Penzberg,
662 Germany). The relative standard curve method was used to obtain the relative quantities
663 of *Oxtr* expression following the manual of Applied Biosystems. To allow the
664 comparation between Koi lines and WT mice, the following primer pair (which can detect
665 the expression of both *mOxtr* and pv*Oxtr*) was used: fr5'-
666 GCCTTTCTTCTTCGTGCAGATG-3' and rv5′-ATGTAGATCCAGGGGTTGCAG-3′ In
667 addition, to specifically detect the expression of pv*Oxtr*, the primer pair fr5′-
668 GCCTTTCTTCTTCGTGCAGATG-3 and rv5'-AAAGAGGTGGCCCGTGAAC-3′ was
669 used in the 2nd qRT-PCR experiment. GAPDH was used as the endogenous control for
670 both experiments and was amplified by the following primer pair: fr5'-
671 GGGTTCCTATAAATACGGACTGC-3' and rv5'- CCATTTTGTCTACGGGACGA-3'.
672 Samples were analyzed in triplicates. A non-template control was performed to ensure
673 that there was no amplification of genomic DNA. All of the experimenters were blind to
674 the genotype of the subjects.
675

Partner preference test (PPT)

Subjects were housed with 4 age-matched and same-sex littermates until testing at adulthood (2-5 months old). 12-14 homozygous? mice were tested for each group. Ovariectomized females were paired and cohoused with a sexually experienced adult wildtype male for 21 days before PPT test. The female was injected with estradiol benzoate (10 μg and 5 μg at 48 h and 24 h before induced mating) and progesterone (500 μg at 4–7 h before induced mating) to ensure high sexual receptivity before mating. Mating was induced on Day 2,9 and16. PPT data was analyzed using TimeSSI1 for social interaction test system (O' Hara & Co., Ltd.). Briefly, the experimental subject was placed in a chamber, in which two pen-boxes (diameter 8cm, height10cm) were located at two diagonally opposite corners. The experimental animal was free to move throughout the chamber and the time spent in close proximity to each pen-box (stay time) is recorded using an automated mouse tracking system (Fig.4 A, B). In the habituation phase, the experimental subject was allowed to explore the chamber for 5 minutes with both pen-boxes empty. In the recognition phase, the partner stimulus animal was restricted in one pen-box, and a novel "stranger" stimulus animal was restricted in another pen-box, and the experimental subject was allowed to explore the chamber for 10 minutes. In the preference phase, the positions of the partner stimulus animal and the "stranger" stimulus

animal were switched, and the experimental subject was allowed to explore the chamber for 20 minutes. To assure unbiased design, pen-box assignments were counterbalanced for the diagonal positions. All of the experimenters were blind to the genotype of the subjects.

Parental behavior test

To examine maternal behavior, we performed pup retrieval test with virgin female mice (2- to 4-months old, 15-18mice/line), following the method described in (Stolzenberg, Stevens, & Rissman, 2012) with some modifications. Briefly, 5 days prior to the behavioral testing, each subject was isolated and housed in separate home cages in the test room. Nesting material (about 1.5 g of cotton wool) was provided for nest making. The tests were conducted in the dark phase of light/dark cycle (12 hours/12 hours). On the day of the test, each subject was placed in the recording area and allowed 15 minutes for habituation. The stimulus pups (age: P2-P3) were collected from a group of donor mothers immediately before the start of the experiment. A retrieval test began with the placement of 3 stimulus pups on the side farthest form the nest, and the female's behavior was recorded by an ARNAN 4 channel security system for 15 minutes. Pup retrieval was defined as picking up the pup and bringing it to the nest. If the subject did not complete

712 the retrieval for 3 pups in 15 minutes, the video recording time was extended to 30
713 minutes. The latency to retrieve each pup (1st, 2nd, 3rd) and the time spent crouching on
714 the pups were time-stamped and calculated manually. A latency of 1800 seconds was
715 assigned if the pup-retrieval was not completed in 30 minutes. Crouching was defined as
716 the mouse supporting itself in a lactation-position over the pups in the nest. Crouching
717 time on a single pup, two pups, and three pups were summed up as total crouching time.
718 All of the experimenters were blind to the genotype of the subjects.
719

720 **3D chromatin verification on Hi-C datasets of humans and mice**

721 The 3D genome structure tracks were obtained from 4DNucleome Consortium
722 (https://www.4dnucleome.org/) where datasets were systematically reanalyzed following
723 recommended standard protocols. The datasets IDs and sample information are provided
724 in the supplementary material (Supplementary Table1,2). 3D Genome Browser(Wang et
725 al., 2018) and WashU Epigenome Browser(Li et al., 2022) were employed for
726 visualizations.
727
728

Experimental design and statistical analysis

The sample sizes were determined by G*Power 3 program (Faul, Erdfelder, Lang, & Buchner, 2007) based on pilot experiments. They are also within the range that is generally accepted in the field. All experiments were performed and analyzed blind to the genotypes and no data point was excluded. All reported sample numbers (n) represent independent biological replicates that are the numbers of tested mice or tissue. All the statistical analyses were performed by SPSS21(IBM). Mixed ANOVA was used for analyzing PPT data and pup retrieval data. Mauchly's test of sphericity was used to test whether or not the assumption of sphericity was met in repeated measures. Greenhouse-Geisser correction was applied when the sphericity was violated. Two-way ANOVA was used for analyzing qRT-PCR region specific data across different mouse lines. One-way ANOVA was used for analyzing crouching time in the parental behavioral test. If there was a significant main effect of an independent factor, post hoc test was used to do multiple comparisons. If there was a significant interaction between within-subject factor and between-subject factor, post hoc pairwise comparisons were applied to analyze the simple main effects. Bonferroni correction was used for all the post hoc tests.

Acknowledgements

This work was supported by the RIKEN Incentive Research Project (100226201701100443) to Q.Z., the Brain Science Project, Center for novel science initiatives, National institutes of natural sciences (BS291003) to Q.Z., the RIKEN Aging Project (10026-201701100263-340120) to Q.Z., the JSPS Kakenhi Grant-in-Aid for Young Scientists (17K18362) to Q.Z., the JSPS Kakenhi Grant-in-Aid for Challenging Research (19K21807) to Q.Z., the JSPS Kakenhi Grant-in-Aid for Challenging Research (22K19478)to Q.Z., the JSPS Kakenhi Grant-in-Aid for Scientific Research (25K10198) to Q.Z., the Takeda Medical Research Grant to Q.Z., the International Education and Research Laboratory Program of University of Tsukuba to L.Y. and Q.Z.. We thank Dr. Katsuhiko Nishimori (Tohoku University and Fukushima Medical University, Japan) for providing *mOxtr*-Ires-Cre knock-in line and *mOxtr*-/- mutant line; Dr. Cary Lai (Indiana University, USA), Dr. Takuji Iwasato(National Institute of Genetics, Japan) and Dr. Seiya Mizuno(University of Tsukuba, Japan) for their advice on BAC vector construction; Dr. Volkhard Maeckel (CERN, Switzerland) for helping with image capturing; Dr. Yong Zhang (Tongji University, China) for the stimulating discussion about 3D chromatin structure, and we thank the Laboratory of Animal Resource Center of University of Tsukuba for pronuclear injection.

765

766 **Author Contributions:**

767 Q.Z. and L.Y. conceived and designed the study. Q.Z., M.T., L.N., K.I., L.K., M.P., Y.N.,

768 M.S., and T.S. performed experiments. Q.Z., M.T., L.N., K.I., L.K., M.P., and K.N.

769 analyzed data. S.I. provided guidance and facilities for transgene vector construction.

770 Q.Z. and L.Y. supervised the project and wrote the manuscript. All authors contributed to

771 discussion and approved the final version.

772

773

774

775

776

777

778

779

780

781

782

783 **References:**

784 Ahern, T. H., Olsen, S., Tudino, R., & Beery, A. K. (2021). Natural variation in the oxytocin
785 receptor gene and rearing interact to influence reproductive and nonreproductive social
786 behavior and receptor binding. *Psychoneuroendocrinology, 128*, 105209.
787 doi:10.1016/j.psyneuen.2021.105209

788 Amadei, E. A., Johnson, Z. V., Jun Kwon, Y., Shpiner, A. C., Saravanan, V., Mays, W. D., . . . Liu,
789 R. C. (2017). Dynamic corticostriatal activity biases social bonding in monogamous
790 female prairie voles. *Nature, 546*(7657), 297-301. doi:10.1038/nature22381

791 Barrett, C. E., Arambula, S. E., & Young, L. J. (2015). The oxytocin system promotes resilience to
792 the effects of neonatal isolation on adult social attachment in female prairie voles. *Transl*
793 *Psychiatry, 5*(7), e606. doi:10.1038/tp.2015.73

794 Beagan, J. A., & Phillips-Cremins, J. E. (2020). On the existence and functionality of topologically
795 associating domains. *Nature Genetics, 52*(1), 8-16. doi:10.1038/s41588-019-0561-1

796 Beil, J., Fairbairn, L., Pelczar, P., & Buch, T. (2012). Is BAC transgenesis obsolete? State of the
797 art in the era of designer nucleases. *J Biomed Biotechnol, 2012*, 308414.
798 doi:10.1155/2012/308414

Bian, Q., & Belmont, A. S. (2010). BAC TG-EMBED: one-step method for high-level, copy-number-dependent, position-independent transgene expression. *Nucleic Acids Research, 38*(11), e127-e127. doi:10.1093/nar/gkq178

Carcea, I., Caraballo, N. L., Marlin, B. J., Ooyama, R., Riceberg, J. S., Mendoza Navarro, J. M., . . . Froemke, R. C. (2021). Oxytocin neurons enable social transmission of maternal behaviour. *Nature, 596*(7873), 553-557. doi:10.1038/s41586-021-03814-7

Chandler, K. J., Chandler, R. L., Broeckelmann, E. M., Hou, Y., Southard-Smith, E. M., & Mortlock, D. P. (2007). Relevance of BAC transgene copy number in mice: transgene copy number variation across multiple transgenic lines and correlations with transgene integrity and expression. *Mamm Genome, 18*(10), 693-708. doi:10.1007/s00335-007-9056-y

Chen, Z., Han, Y., Ma, Z., Wang, X., Xu, S., Tang, Y., . . . Zhan, Y. (2024). A prefrontal-thalamic circuit encodes social information for social recognition. *Nature Communications, 15*(1), 1036. doi:10.1038/s41467-024-45376-y

Crook, Z. R., & Housman, D. (2011). Huntington's disease: can mice lead the way to treatment? *Neuron, 69*(3), 423-435. doi:10.1016/j.neuron.2010.12.035

Dekker, J., Rippe, K., Dekker, M., & Kleckner, N. (2002). Capturing chromosome conformation. *Science, 295*(5558), 1306-1311. doi:10.1126/science.1067799

Dixon, J. R., Selvaraj, S., Yue, F., Kim, A., Li, Y., Shen, Y., . . . Ren, B. (2012). Topological domains in mammalian genomes identified by analysis of chromatin interactions. *Nature, 485*(7398), 376-380. doi:10.1038/nature11082

Faul, F., Erdfelder, E., Lang, A. G., & Buchner, A. (2007). G*Power 3: a flexible statistical power analysis program for the social, behavioral, and biomedical sciences. *Behav Res Methods, 39*(2), 175-191. doi:10.3758/bf03193146

Ferrante, R. J. (2009). Mouse models of Huntington's disease and methodological considerations for therapeutic trials. *Biochimica et Biophysica Acta (BBA) - Molecular Basis of Disease, 1792*(6), 506-520. doi:https://doi.org/10.1016/j.bbadis.2009.04.001

Froemke, R. C., & Young, L. J. (2021). Oxytocin, Neural Plasticity, and Social Behavior. *Annu Rev Neurosci, 44*, 359-381. doi:10.1146/annurev-neuro-102320-102847

Gerfen, C. R., Paletzki, R., & Heintz, N. (2013). GENSAT BAC cre-recombinase driver lines to study the functional organization of cerebral cortical and basal ganglia circuits. *Neuron, 80*(6), 1368-1383. doi:10.1016/j.neuron.2013.10.016

Gibcus, Johan H., & Dekker, J. (2013). The Hierarchy of the 3D Genome. *Molecular Cell, 49*(5), 773-782. doi:https://doi.org/10.1016/j.molcel.2013.02.011

833 Gilligan, P., Brenner, S., & Venkatesh, B. (2003). Neurone-specific expression and regulation of
834 the pufferfish isotocin and vasotocin genes in transgenic mice. *J Neuroendocrinol, 15*(11),
835 1027-1036. doi:10.1046/j.1365-2826.2003.01090.x
836 Gong, S., Doughty, M., Harbaugh, C. R., Cummins, A., Hatten, M. E., Heintz, N., & Gerfen, C. R.
837 (2007). Targeting Cre recombinase to specific neuron populations with bacterial artificial
838 chromosome constructs. *J Neurosci, 27*(37), 9817-9823. doi:10.1523/jneurosci.2707-
839 07.2007
840 Gong, S., Zheng, C., Doughty, M. L., Losos, K., Didkovsky, N., Schambra, U. B., . . . Heintz, N.
841 (2003). A gene expression atlas of the central nervous system based on bacterial artificial
842 chromosomes. *Nature, 425*(6961), 917-925. doi:10.1038/nature02033
843 Grinevich, V., Knobloch-Bollmann, H. S., Eliava, M., Busnelli, M., & Chini, B. (2016). Assembling
844 the Puzzle: Pathways of Oxytocin Signaling in the Brain. *Biol Psychiatry, 79*(3), 155-164.
845 doi:10.1016/j.biopsych.2015.04.013
846 Heintz, N. (2004). Gene Expression Nervous System Atlas (GENSAT). *Nature Neuroscience,*
847 *7*(5), 483-483. doi:10.1038/nn0504-483
848 Hidema, S., Fukuda, T., Hiraoka, Y., Mizukami, H., Hayashi, R., Otsuka, A., . . . Nishimori, K.
849 (2016). Generation of Oxtr cDNA(HA)-Ires-Cre Mice for Gene Expression in an

Oxytocin Receptor Specific Manner. *J Cell Biochem, 117*(5), 1099-1111. doi:10.1002/jcb.25393

Inoue, K., Ford, C. L., Horie, K., & Young, L. J. (2022). Oxytocin receptors are widely distributed in the prairie vole (Microtus ochrogaster) brain: Relation to social behavior, genetic polymorphisms, and the dopamine system. *Journal of Comparative Neurology, 530*(16), 2881-2900. doi:https://doi.org/10.1002/cne.25382

Jurek, B., & Neumann, I. D. (2018). The Oxytocin Receptor: From Intracellular Signaling to Behavior. *Physiological reviews, 98*(3), 1805-1908. doi:10.1152/physrev.00031.2017

Kandasamy, L. C., Tsukamoto, M., Banov, V., Tsetsegee, S., Nagasawa, Y., Kato, M., . . . Zhang, Q. (2021). Limb-clasping, cognitive deficit and increased vulnerability to kainic acid-induced seizures in neuronal glycosylphosphatidylinositol deficiency mouse models. *Human Molecular Genetics, 30*(9), 758-770. doi:10.1093/hmg/ddab052

Kappel, J. M., Förster, D., Slangewal, K., Shainer, I., Svara, F., Donovan, J. C., . . . Larsch, J. (2022). Visual recognition of social signals by a tectothalamic neural circuit. *Nature, 608*(7921), 146-152. doi:10.1038/s41586-022-04925-5

Kim, J. H., Lee, S. R., Li, L. H., Park, H. J., Park, J. H., Lee, K. Y., . . . Choi, S. Y. (2011). High cleavage efficiency of a 2A peptide derived from porcine teschovirus-1 in human cell lines, zebrafish and mice. *PloS one, 6*(4), e18556. doi:10.1371/journal.pone.0018556

King, L. B., Walum, H., Inoue, K., Eyrich, N. W., & Young, L. J. (2016). Variation in the Oxytocin Receptor Gene Predicts Brain Region-Specific Expression and Social Attachment. *Biol Psychiatry, 80*(2), 160-169. doi:10.1016/j.biopsych.2015.12.008

Leng, G., & Ludwig, M. (2008). Neurotransmitters and peptides: whispered secrets and public announcements. *J Physiol, 586*(23), 5625-5632. doi:10.1113/jphysiol.2008.159103

Li, D., Purushotham, D., Harrison, J. K., Hsu, S., Zhuo, X., Fan, C., . . . Wang, T. (2022). WashU Epigenome Browser update 2022. *Nucleic Acids Research, 50*(W1), W774-W781. doi:10.1093/nar/gkac238

Lieberman-Aiden, E., van Berkum, N. L., Williams, L., Imakaev, M., Ragoczy, T., Telling, A., . . . Dekker, J. (2009). Comprehensive Mapping of Long-Range Interactions Reveals Folding Principles of the Human Genome. *Science, 326*(5950), 289-293. doi:doi:10.1126/science.1181369

Mack, K. L., Campbell, P., & Nachman, M. W. (2016). Gene regulation and speciation in house mice. *Genome Res, 26*(4), 451-461. doi:10.1101/gr.195743.115

Marlin, B. J., Mitre, M., D'Amour J, A., Chao, M. V., & Froemke, R. C. (2015). Oxytocin enables maternal behaviour by balancing cortical inhibition. *Nature, 520*(7548), 499-504. doi:10.1038/nature14402

McGraw, L. A., Davis, J. K., Lowman, J. J., ten Hallers, B. F. H., Koriabine, M., Young, L. J., . . . Thomas, J. W. (2010). Development of genomic resources for the prairie vole (Microtus ochrogaster): construction of a BAC library and vole-mouse comparative cytogenetic map. *BMC Genomics, 11*(1), 70. doi:10.1186/1471-2164-11-70

McGraw, L. A., Davis, J. K., Thomas, P. J., Young, L. J., & Thomas, J. W. (2012). BAC-based sequencing of behaviorally-relevant genes in the prairie vole. *PloS one, 7*(1), e29345. doi:10.1371/journal.pone.0029345

Mitre, M., Marlin, B. J., Schiavo, J. K., Morina, E., Norden, S. E., Hackett, T. A., . . . Froemke, R. C. (2016). A Distributed Network for Social Cognition Enriched for Oxytocin Receptors. *J Neurosci, 36*(8), 2517-2535. doi:10.1523/jneurosci.2409-15.2016

Newmaster, K. T., Nolan, Z. T., Chon, U., Vanselow, D. J., Weit, A. R., Tabbaa, M., . . . Kim, Y. (2020). Quantitative cellular-resolution map of the oxytocin receptor in postnatally developing mouse brains. *Nature Communications, 11*(1), 1885. doi:10.1038/s41467-020-15659-1

Olazábal, D. E., & Young, L. J. (2006). Oxytocin receptors in the nucleus accumbens facilitate "spontaneous" maternal behavior in adult female prairie voles. *Neuroscience, 141*(2), 559-568. doi:10.1016/j.neuroscience.2006.04.017

Osada, N., Miyagi, R., & Takahashi, A. (2017). Cis- and Trans-regulatory Effects on Gene Expression in a Natural Population of Drosophila melanogaster. *Genetics, 206*(4), 2139-2148. doi:10.1534/genetics.117.201459

Parmaksiz, D., & Kim, Y. (2025). Navigating Central Oxytocin Transport: Known Realms and Uncharted Territories. *Neuroscientist, 31*(3), 234-261. doi:10.1177/10738584241268754

Phelps, S. M., & Young, L. J. (2003). Extraordinary diversity in vasopressin (V1a) receptor distributions among wild prairie voles (Microtus ochrogaster): patterns of variation and covariation. *J Comp Neurol, 466*(4), 564-576. doi:10.1002/cne.10902

Rajderkar, S., Barozzi, I., Zhu, Y., Hu, R., Zhang, Y., Li, B., . . . Pennacchio, L. A. (2023). Topologically associating domain boundaries are required for normal genome function. *Communications Biology, 6*(1), 435. doi:10.1038/s42003-023-04819-w

Rangel, M. J., Baldo, M. V. C., & Canteras, N. S. (2018). Influence of the anteromedial thalamus on social defeat-associated contextual fear memory. *Behavioural Brain Research, 339*, 269-277. doi:https://doi.org/10.1016/j.bbr.2017.10.038

Rigney, N., de Vries, G. J., Petrulis, A., & Young, L. J. (2022). Oxytocin, Vasopressin, and Social Behavior: From Neural Circuits to Clinical Opportunities. *Endocrinology, 163*(9). doi:10.1210/endocr/bqac111

Rogers Flattery, C. N., Coppeto, D. J., Inoue, K., Rilling, J. K., Preuss, T. M., & Young, L. J. (2022). Distribution of brain oxytocin and vasopressin V1a receptors in chimpanzees (Pan troglodytes): comparison with humans and other primate species. *Brain Struct Funct, 227*(5), 1907-1919. doi:10.1007/s00429-021-02369-7

Ross, H. E., Freeman, S. M., Spiegel, L. L., Ren, X., Terwilliger, E. F., & Young, L. J. (2009). Variation in oxytocin receptor density in the nucleus accumbens has differential effects on affiliative behaviors in monogamous and polygamous voles. *J Neurosci, 29*(5), 1312-1318. doi:10.1523/jneurosci.5039-08.2009

Ross, H. E., & Young, L. J. (2009). Oxytocin and the neural mechanisms regulating social cognition and affiliative behavior. *Front Neuroendocrinol, 30*(4), 534-547. doi:10.1016/j.yfrne.2009.05.004

Schmidt, E. F., Kus, L., Gong, S., & Heintz, N. (2013). BAC transgenic mice and the GENSAT database of engineered mouse strains. *Cold Spring Harb Protoc, 2013*(3). doi:10.1101/pdb.top073692

Shenoy, S. A., Zheng, S., Liu, W., Dai, Y., Liu, Y., Hou, Z., . . . Li, C. (2022). A novel and accurate full-length HTT mouse model for Huntington's disease. *eLife, 11*, e70217. doi:10.7554/eLife.70217

Shi, X., Ng, D. W. K., Zhang, C., Comai, L., Ye, W., & Jeffrey Chen, Z. (2012). Cis- and trans-regulatory divergence between progenitor species determines gene-expression novelty in Arabidopsis allopolyploids. *Nature Communications, 3*(1), 950. doi:10.1038/ncomms1954

Signor, S. A., & Nuzhdin, S. V. (2018). The Evolution of Gene Expression in cis and trans. *Trends Genet, 34*(7), 532-544. doi:10.1016/j.tig.2018.03.007

Skuse, D. H., Lori, A., Cubells, J. F., Lee, I., Conneely, K. N., Puura, K., . . . Young, L. J. (2014). Common polymorphism in the oxytocin receptor gene (OXTR) is associated with human social recognition skills. *Proceedings of the National Academy of Sciences, 111*(5), 1987-1992. doi:doi:10.1073/pnas.1302985111

Smirnov, A., Fishman, V., Yunusova, A., Korablev, A., Serova, I., Skryabin, B. V., . . . Battulin, N. (2019). DNA barcoding reveals that injected transgenes are predominantly processed by homologous recombination in mouse zygote. *Nucleic Acids Research, 48*(2), 719-735. doi:10.1093/nar/gkz1085

Stolzenberg, D. S., Stevens, J. S., & Rissman, E. F. (2012). Experience-facilitated improvements in pup retrieval; evidence for an epigenetic effect. *Horm Behav, 62*(2), 128-135. doi:10.1016/j.yhbeh.2012.05.012

Suster, M. L., Abe, G., Schouw, A., & Kawakami, K. (2011). Transposon-mediated BAC transgenesis in zebrafish. *Nature Protocols, 6*(12), 1998-2021. doi:10.1038/nprot.2011.416

Taguchi, T., Ikuno, M., Hondo, M., Parajuli, L. K., Taguchi, K., Ueda, J., . . . Takahashi, R. (2019). α-Synuclein BAC transgenic mice exhibit RBD-like behaviour and hyposmia: a prodromal Parkinson's disease model. *Brain, 143*(1), 249-265. doi:10.1093/brain/awz380

Takayanagi, Y., Yoshida, M., Bielsky, I. F., Ross, H. E., Kawamata, M., Onaka, T., . . . Nishimori, K. (2005). Pervasive social deficits, but normal parturition, in oxytocin receptor-deficient mice. *Proceedings of the National Academy of Sciences, 102*(44), 16096-16101. doi:doi:10.1073/pnas.0505312102

Theofanopoulou, C., Andirkó, A., Boeckx, C., & Jarvis, E. D. (2022). Oxytocin and vasotocin receptor variation and the evolution of human prosociality. *Comprehensive Psychoneuroendocrinology, 11*, 100139. doi:https://doi.org/10.1016/j.cpnec.2022.100139

Venkatesh, B., Si-Hoe, S. L., Murphy, D., & Brenner, S. (1997). Transgenic rats reveal functional conservation of regulatory controls between the Fugu isotocin and rat oxytocin genes. *Proc Natl Acad Sci U S A, 94*(23), 12462-12466. doi:10.1073/pnas.94.23.12462

969 Walum, H., & Young, L. J. (2018). The neural mechanisms and circuitry of the pair bond. *Nat Rev*
970 *Neurosci, 19*(11), 643-654. doi:10.1038/s41583-018-0072-6
971 Walum, H., & Young, L. J. (2018). The neural mechanisms and circuitry of the pair bond. *Nature*
972 *Reviews Neuroscience, 19*(11), 643-654. doi:10.1038/s41583-018-0072-6
973 Wang, Y., Song, F., Zhang, B., Zhang, L., Xu, J., Kuang, D., . . . Yue, F. (2018). The 3D Genome
974 Browser: a web-based browser for visualizing 3D genome organization and long-range
975 chromatin interactions. *Genome Biol, 19*(1), 151. doi:10.1186/s13059-018-1519-9
976 Wendt, K. S., Yoshida, K., Itoh, T., Bando, M., Koch, B., Schirghuber, E., . . . Peters, J. M. (2008).
977 Cohesin mediates transcriptional insulation by CCCTC-binding factor. *Nature,*
978 *451*(7180), 796-801. doi:10.1038/nature06634
979 Wolff, M., & Vann, S. D. (2019). The Cognitive Thalamus as a Gateway to Mental
980 Representations. *J Neurosci, 39*(1), 3-14. doi:10.1523/jneurosci.0479-18.2018
981 Xiao, J. Y., Hafner, A., & Boettiger, A. N. (2021). How subtle changes in 3D structure can create
982 large changes in transcription. *eLife, 10*, e64320. doi:10.7554/eLife.64320
983 Yang, X. W., & Lu, X.-H. (2008). Chapter 19 - The Bac Transgenic Approach to Study
984 Parkinson's Disease in Mice. In R. Nass & S. Przedborski (Eds.), *Parkinson's Disease* (pp.
985 247-268). San Diego: Academic Press.

Young, L. J., & Crews, D. (1995). Comparative neuroendocrinology of steroid receptor gene expression and regulation: Relationship to physiology and behavior. *Trends Endocrinol Metab, 6*(9-10), 317-323. doi:10.1016/1043-2760(95)00175-1

Young, L. J., & Zhang, Q. I. (2021). On the Origins of Diversity in Social Behavior. *The Japanese Journal of Animal Psychology, doi: 10.2502/janip.71.1.4*. doi:doi: 10.2502/janip.71.1.4

Zhang, Q., Sano, C., Masuda, A., Ando, R., Tanaka, M., & Itohara, S. (2016). Netrin-G1 regulates fear-like and anxiety-like behaviors in dissociable neural circuits. *Scientific Reports, 6*(1), 28750. doi:10.1038/srep28750

1004 **Figure titles and Legends:**

1005 **Fig.1 Construction of Koi lines.** (A) Example of the remarkable species difference of
1006 brain OXTR distribution. OXTR receptor autoradiography in dorsal caudate putamen
1007 (CP) and nucleus accumbens shell (NAccSh) of rat, mouse, and prairie voleis (Adapted
1008 Froemke and Young(Froemke & Young, 2021)). (B) The pv*Oxtr* BAC clone contains the
1009 entire sequence of pv*Oxtr* gene (colored green), the complete intergenic sequence both
1010 upstream and downstream of pv*Oxtr* gene, the 12th exon of *Rad18* (colored blue) and the
1011 2nd exon of *Cav3* (colored purple). The yellow arrows indicate the direction of
1012 transcription. (C) Schematic diagram of the strategy to generate Koi mice. The P2A-
1013 NLS-Cre-Frt-Amp-Frt cassette was inserted in-frame right before the stop codon of *Oxtr*.
1014 And the ampicillin selection marker was deleted by 706-Flpe. PCR primers for verifying
1015 the targeted alleles are shown as red arrows. (D) Two correctly modified vector clones
1016 were verified by using PCR with p2 and p8. (E) Koi lines were verified by 5 pairs of
1017 primers. From Lane1 to Lane8 are 100bp marker, p3+p7, p2+p6, p2+p7, p4+p8, p2+p8,
1018 blank and 1kb marker.

1019

1020 **Fig.2 Transgenic CRE mediated Lac-Z reporter gene expression in the brain and**
1021 **mammary gland of Koi lines.** X-gal staining of the brains and mammary glands are

1022 from the double positive (*Cre*+, *LacZ*+) offspring from Koi-1 (A, F, K, P), Koi-2 (B, G,
1023 L, Q), Koi-3 (G, H, M, R), Koi-4 (D, I, N, S) and *mOxtr-Ires-Cre* knock-in line (E, J, O,
1024 T). The *mOxtr-Ires-Cre* KI line used contains Cre (and an HA tag) inserted in the third
1025 exon, right after the start codon. Note that regardless of the insertion site of Cre in the
1026 mouse genome DNA or pvOxtr-BAC transgene, *Oxtr* expression visualized by Lac-Z
1027 staining in the mammary gland was comparable between the mOxtr-Ires-Cre KI and Koi
1028 lines. This contrasts with the diverse expression patterns of *Oxtr* expression in the brain.
1029 U, V, M, X, Y are the magnified images of the areas within the yellow-border squares
1030 from D, N, E, J, O, respectively, to show the distribution of low-density Lac-Z positive
1031 cells in these areas. Scale bar=1mm (A-O), 500um (P-T) and 200um (U-Y). (Z) The
1032 estimated copy number of transgene of all Koi lines. See Supplementary Figure 2 for
1033 images of Koi-5-8 lines. PFC=prefrontal cortex, LS=lateral septum, BLA=basolateral
1034 amygdala, VMH=ventromedial nucleus of the hypothalamus, Tha=thalamus.
1035
1036 **Fig.3 The expression of OXTR in adult brain of Koi lines.** Autoradiographs illustrate
1037 the distribution of OXTR binding in adult Koi-1: m*Oxtr*$^{-/-}$ (A, F, K), Koi-2: m*Oxtr*$^{-/-}$ (B,
1038 G, L), Koi-3: m*Oxtr*$^{-/-}$ (C, H, M), Koi-4: m*Oxtr*$^{-/-}$ (D, I, N) and wild type (WT) (E, J, O).
1039 All Koi mice used for this analysis were pv*Oxtr-P2A-Cre*: m*Oxtr*$^{-/-}$ mice in which the

1040 pvOXTR was expressed while endogenous mOXTR was absent. PFC=prefrontal cortex,
1041 LS=lateral septum, BLA=basolateral amgydala, VMH=ventromedial nucleus of the
1042 hypothalamus, Tha=thalamus. Scale bar=1mm.
1043
1044 **Fig.4 mRNA expression of *Oxtr* in the adult brain of Koi lines.** *Oxtr* mRNA (red) was
1045 labeled with in situ hybridization against DAPI for nuclei labelling (purple). (A) and (C)
1046 show clear expression of *Oxtr* in the PFA and Ctx in Koi-3: m*Oxtr*$^{-/-}$. (B) and(D) show
1047 clear expression of *Oxtr* in the NAc and Tha in Koi-4: m*Oxtr*$^{-/-}$. All Koi mice used for this
1048 analysis were pv*Oxtr-P2A-Cre*: m*Oxtr*$^{-/-}$ mice, in which the pvOXTR was expressed
1049 while endogenous mOXTR was absent. PFC=prefrontal cortex, NAc= Nucleus
1050 accumbens, Ctx=Cortex, Tha=thalamus. Scale bar=400um for A and B, 500um for C and
1051 D.
1052
1053 **Fig.5 Quantitative PCR analysis of *Oxtr* mRNA expression in different brain regions**
1054 **of Koi lines. (A)** A primer set recognizing both m*Oxtr* and pv*Oxtr* was used to analyze
1055 *Oxtr* mRNA in olfactory bulb, prefrontal cortex, ventral striatum and thalamus from WT,
1056 Koi-1: m*Oxtr*$^{-/-}$, Koi-2: m*Oxtr*$^{-/-}$, Koi-3: m*Oxtr*$^{-/-}$, Koi-4: m*Oxtr*$^{-/-}$ and *mOxtr*$^{-/-}$ mutant
1057 mice, n=4 for each genotype. Note that the level of *Oxtr* mRNA in *mOxtr*$^{-/-}$ mutant mice

1058 was nondetectable (ND). The autoradiograph of OXTR binding in olfactory bulb from
1059 each line were shown alongside the legend. There was a significant interaction between
1060 position and genotype F (12,64) =26.33, p<0.0001; Post hoc Bonferroni test revealed that
1061 *Oxtr* expression level in olfactory bulb of Koi-1: m*Oxtr*$^{-/-}$ was significantly higher than
1062 that of other genotype groups (p<0.0001 for all), and that of Koi-4: m*Oxtr*$^{-/-}$ was
1063 significantly higher than that of Koi-3: m*Oxtr*$^{-/-}$ p<0.05. And the striatum of Koi-4:
1064 m*Oxtr*$^{-/-}$ expressed significantly higher *Oxtr* when compared with WT and Koi-3: m*Oxtr*$^{-/-}$
1065 (p<0.05 for both). The *Oxtr* expression level in thalamus of Koi-4: m*Oxtr*$^{-/-}$ was
1066 significantly higher than other genotype groups (p<0.0001 when compared with WT and
1067 Koi-3: m*Oxtr*$^{-/-}$, p<0.001 when compared with Koi-2: m*Oxtr*$^{-/-}$, p<0.05 when compared
1068 with Koi-1: m*Oxtr*$^{-/-}$) (B) A primer set specifically recognizing pv*Oxtr.* was used to
1069 analyze *Oxtr* mRNA in WT, Koi-1: m*Oxtr*$^{-/-}$, Koi-2: m*Oxtr*$^{-/-}$, Koi-3: m*Oxtr*$^{-/-}$ and Koi-4:
1070 m*Oxtr*$^{-/-}$ mic, n=4 for each genotype. Note that the level of *Oxtr* mRNA in WT mice was
1071 barely detectable. There was a significant interaction between position and genotype F
1072 (9,48) =89.25, p<0.0001; Post Hoc Bonferroni test revealed that *Oxtr* expression level in
1073 the olfactory bulb of Koi-1: m*Oxtr*$^{-/-}$ was significantly higher than that of other genotype
1074 groups (p<0.0001 for all), and that of Koi-4: m*Oxtr*$^{-/-}$ was significantly higher than that of
1075 Koi-2: m*Oxtr*$^{-/-}$ and Koi-3: m*Oxtr*$^{-/-}$ (p<0.0001 for both). The *Oxtr* expression level in

1076 prefrontal cortex of Koi-3: m*Oxtr*$^{-/-}$ was significantly higher than that of other groups

1077 ($p<0.01$ when comparing with Koi-1: m*Oxtr*$^{-/-}$ and Koi-4: m*Oxtr*$^{-/-}$; $p<0.05$ when

1078 comparing with Koi-2: m*Oxtr*$^{-/-}$). And the striatum of Koi-4: m*Oxtr*$^{-/-}$ expressed

1079 significantly higher *Oxtr* when comparing with Koi-2: m*Oxtr*$^{-/-}$ and Koi-3: m*Oxtr*$^{-/-}$

1080 ($p<0.01$ for both). The *Oxtr* expression level in thalamus of Koi-4: m*Oxtr*$^{-/-}$ was

1081 significantly higher than that of other genotype groups ($p<0.0001$ for all). All Koi mice

1082 used for this analysis were pv*Oxtr-P2A-Cre*: m*Oxtr*$^{-/-}$ mice, in which the pvOXTR was

1083 expressed while endogenous mOXTR was absent. The significance of interaction

1084 between genotype and brain region: # # # # $p<0.0001$. The significance of single main

1085 effect of genotype: * $p<0.05$; * * $p<0.01$; * * * $p<0.001$; * * * * $p<0.0001$.

1086

1087 **Fig.6 Social behaviors of Koi lines.** (A) Illustration of the partner preference test (PPT)

1088 paradigm. The experimental mouse was placed in a chamber with an automatic

1089 monitoring system, where it could freely explore two pen-boxes localized in two diagonal

1090 corners. Habituation phase: two pen-boxes are empty. Recognition phase: a stimulating

1091 partner mouse is placed into one pen-box and a stimulating stranger mouse is placed in

1092 the other one. Preference phase: The positions of two stimulating mice are switched. (B)

1093 Representative traces of one experimental mouse during the three phases. (C-E) The stay

1094 time in the surrounding area of each pen box during three phases;(C) Habituation

1095 phase;(D) Recognition phase; (E) Preference phase. Samples sizes for the PPT are wild

1096 type(WT) (n=12), Koi-1: m*Oxtr*$^{-/-}$ (n=14), Koi-2: m*Oxtr*$^{-/-}$ (n=13) Koi-3: m*Oxtr*$^{-/-}$ (n=12)

1097 Koi-4 : m*Oxtr*$^{-/-}$ (n=14). All the experimental mice are female. (F) The illustration of the

1098 procedure of the maternal behavior test. (G) Pup retrieval latency and (H) crouching time

1099 were recorded and analyzed. Sample sizes for the maternal behavior tests are WT (n=15),

1100 Koi-3: m*Oxtr*$^{-/-}$ (n=18), Koi-4: m*Oxtr*$^{-/-}$ (n=18). Significance of interaction between

1101 independent factors: # $p<0.05$; # # $p<0.01$. Significance of main effect or single main

1102 effect of genotype: * $p<0.05$; * * $p<0.01$; * * * $p<0.001$; * * * *

1103 $p<0.0001$.(Illustrations created with Biorender.com). All Koi mice used for this analysis

1104 were pv*Oxtr-P2A-Cre*: m*Oxtr*$^{-/-}$ mice in which the pvOXTR was expressed while

1105 endogenous mOXTR was absent.

1106

1107 **Fig.7 Heatmap of the chromatin contacts surrounding *Oxtr* and *Oxt* across mouse**

1108 **tissues/cells from megabase-size visualization.** (A) Heatmap of the chromatin contacts

1109 surrounding *Oxtr* across mouse tissues/cells: *Oxtr* is located at a TAD boundary region.

1110 The increase of interactions characterizes the TADs structure and the interaction of two

1111 neighboring TADs can be more clearly observed in brain-related samples. Blue dashed

1112 lines were prepared to help observing the TAD structures, and black circles were prepared

1113 to help observing the long-distance interaction obtained from Hi-C interaction matrices

1114 surrounding *Oxtr*. (B) Heatmap of the chromatin contacts surrounding *Oxt* across mouse

1115 tissues/cells. No TAD structure was observed surrounding *Oxt* locus.

1116

Figures

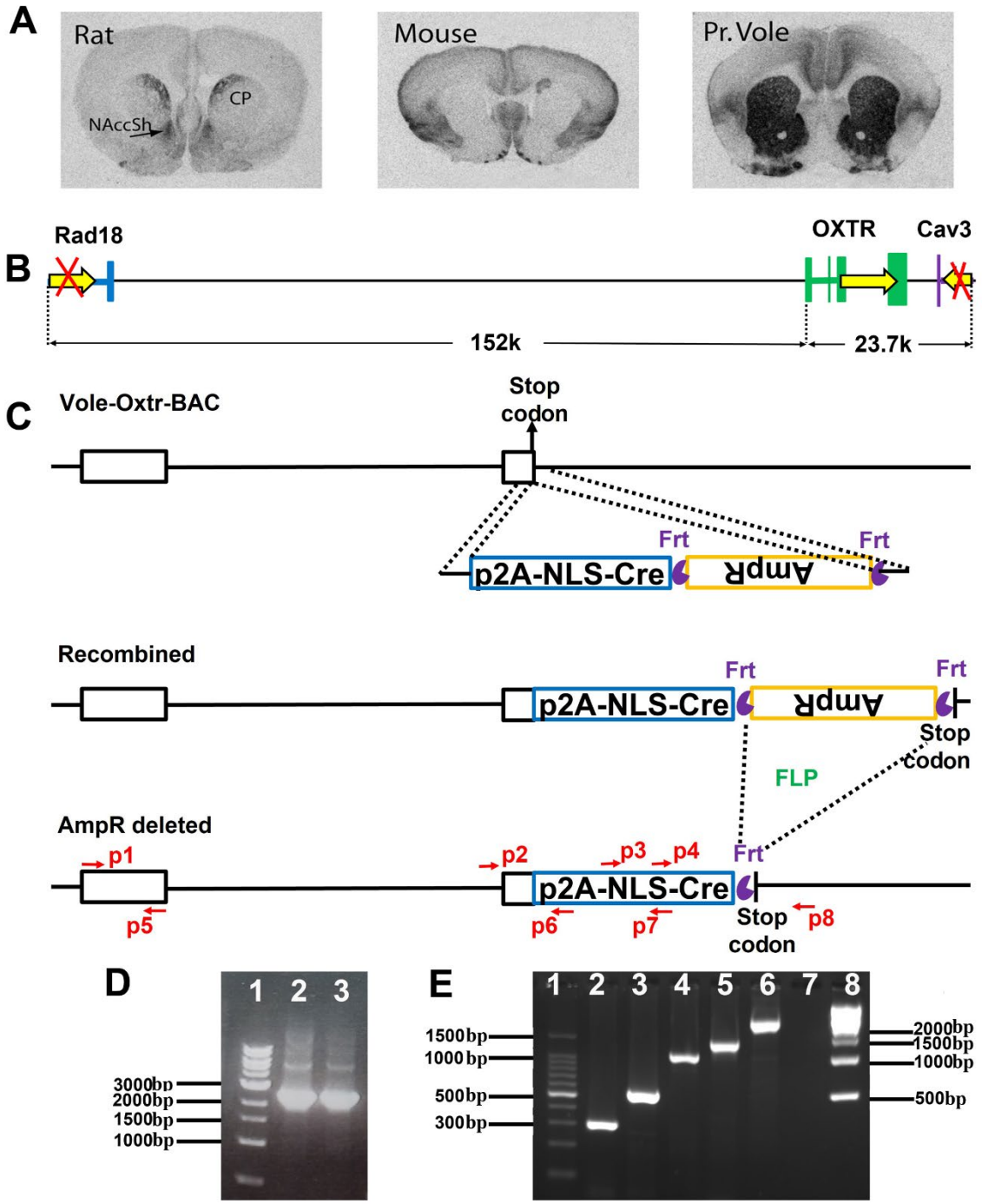

Fig.1 The construction of Koi lines

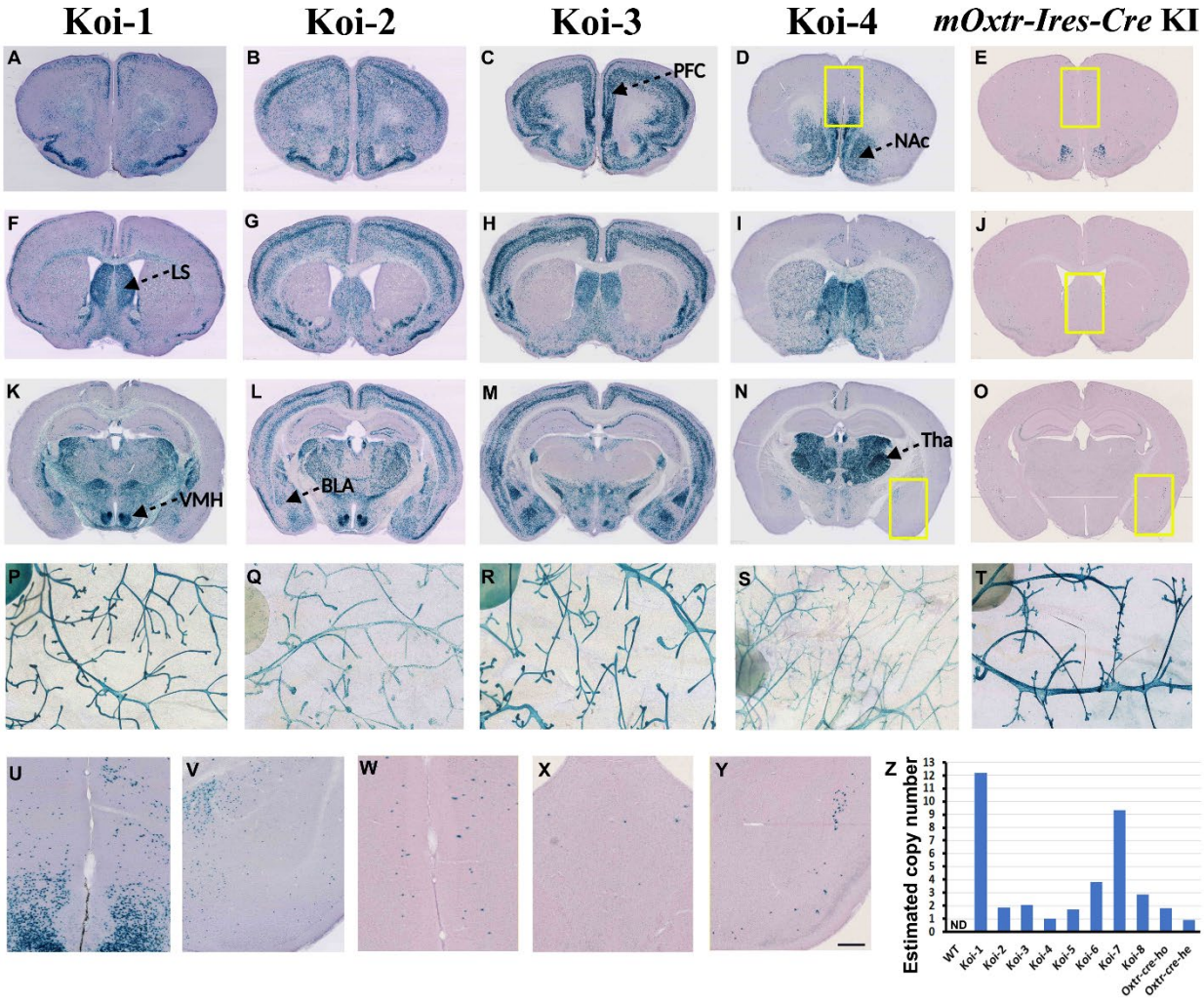

Fig.2 Transgenic CRE mediated Lac-Z reporter gene expression in the brain and mammary gland of Koi line

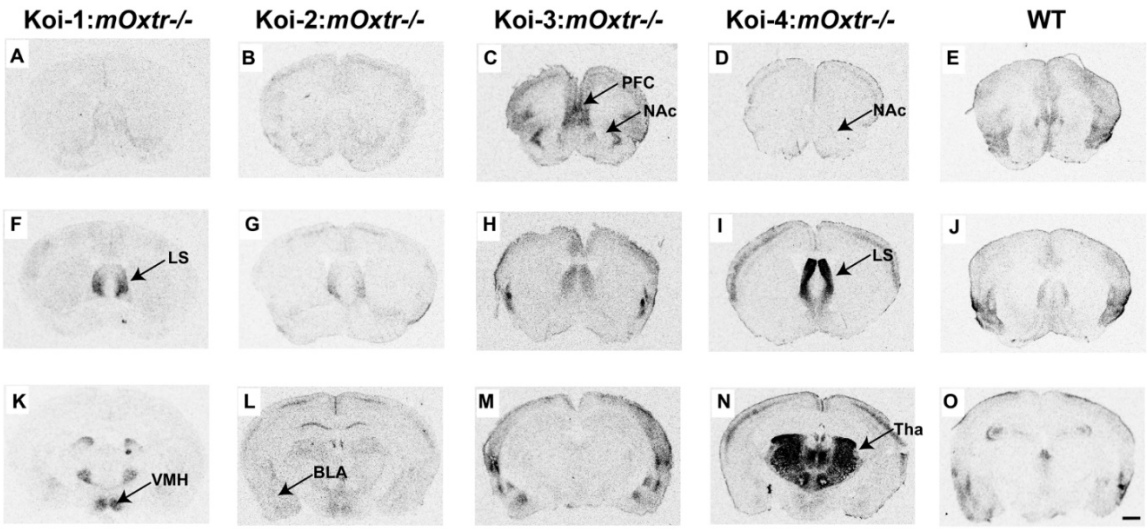

Fig.3The expression of OXTR in the brain of Koi lines.

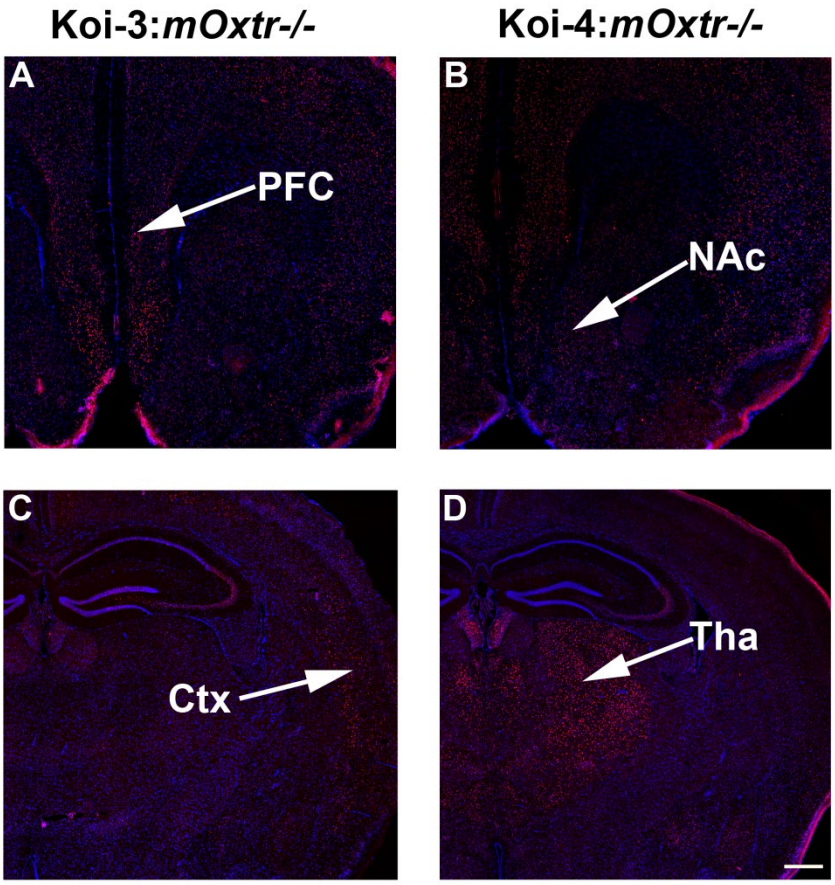

Fig.4 mRNA expression of *Oxtr* in the adult brain of Koi lines.

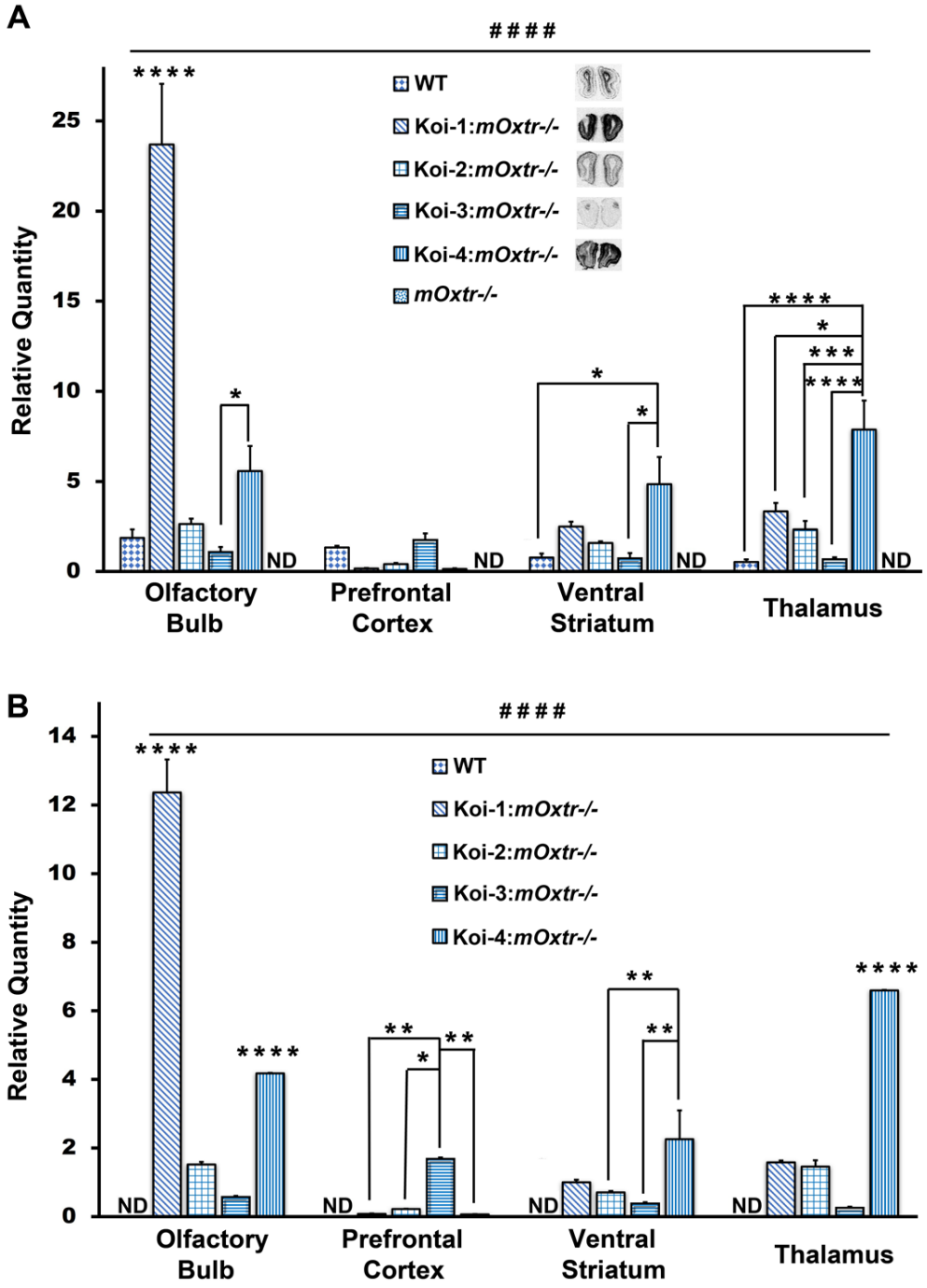

Fig.5 Quantitative PCR analysis of *Oxtr* mRNA expression in different brain regions of Koi lines.

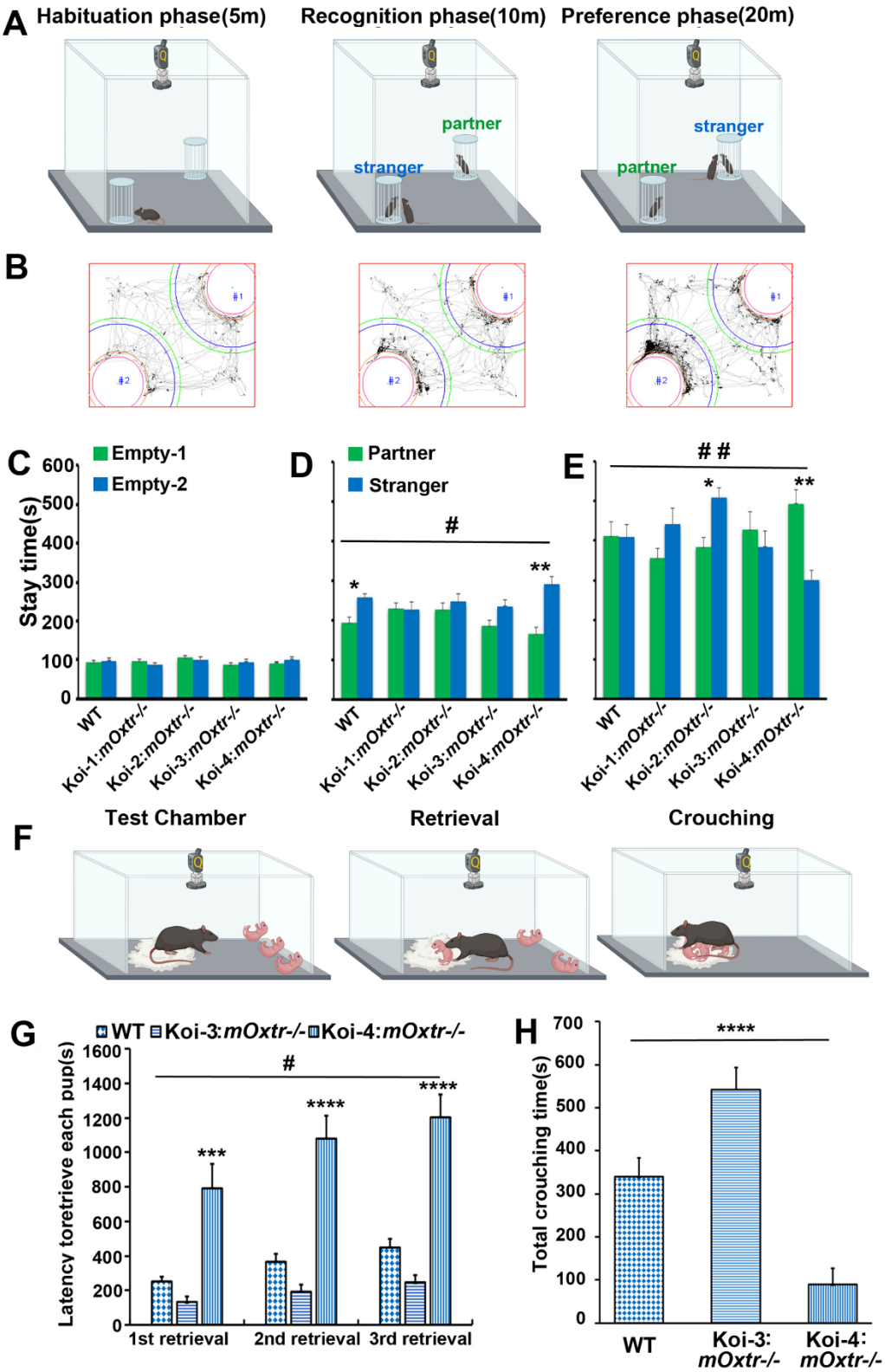

Fig.6 Social behaviors of Koi lines.

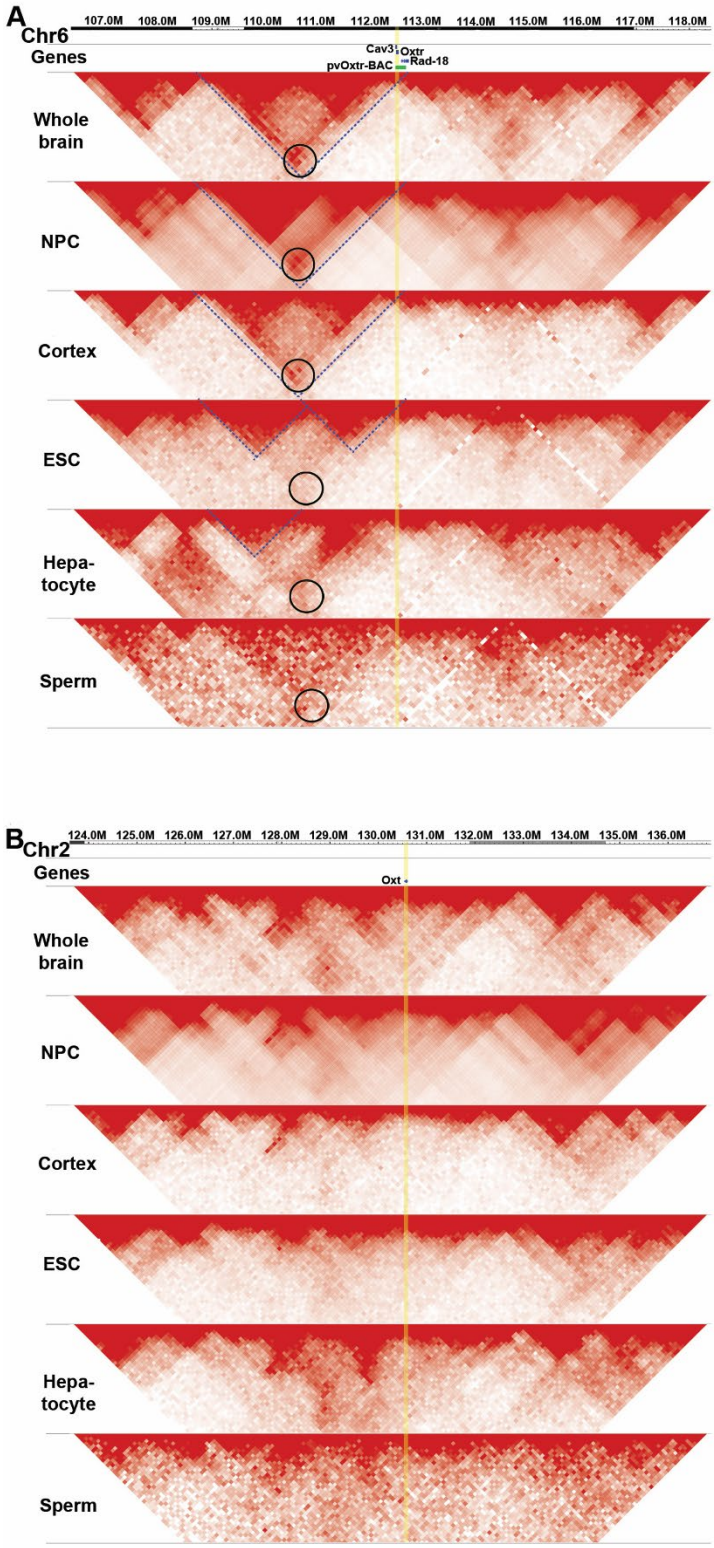

Fig.7 Heatmap of the chromatin contacts surrounding *Oxtr* and *Oxt* across mouse tissues/cells from megabase-size visualization.

Supplementary Information

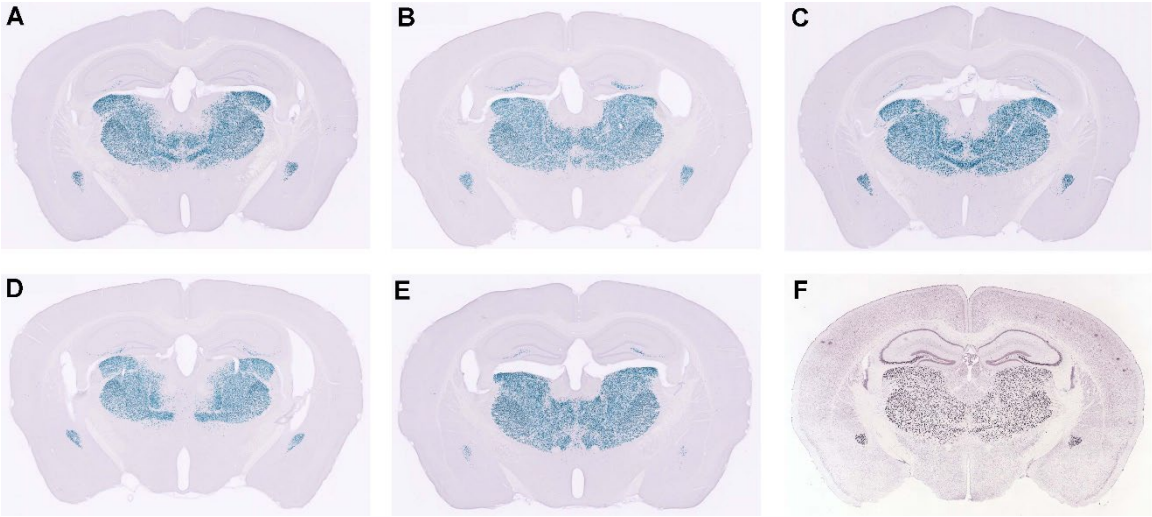

Supplementary Fig.1 Expression pattern of the *Pkcd-Cre* BAC transgene.

All five independent *Pkcd-Cre* BAC transgenic mouse lines (A–E) exhibited expression patterns that closely resembled the endogenous *Pkcd* expression, as shown by in situ hybridization (F). The *Pkcd-Cre* BAC construct was generated using the same strategy as that employed for the Koi lines, incorporating the entire intergenic regions both upstream and downstream of the *Pkcd* gene.

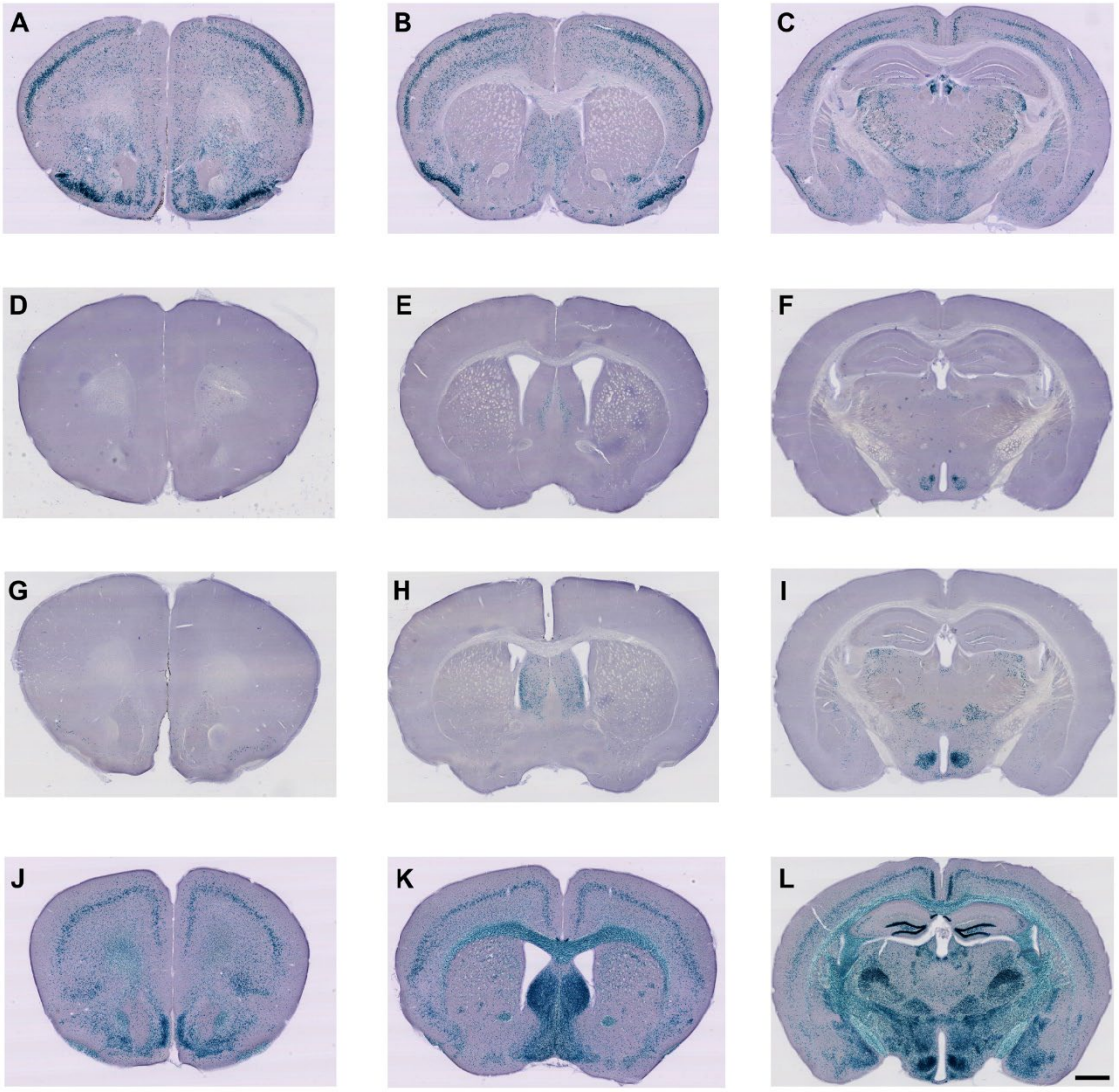

Supplementary Fig.2 Transgenic CRE mediated Lac-Z reporter gene expression in the brain of Koi lines. X-gal staining of the brains from the double positive (*Cre*+, *LacZ*+) offspring of Koi-5 (A-C), Koi-6 (D-F), Koi-7 (G-I), Koi-8 (J-L). Scale bar=1mm

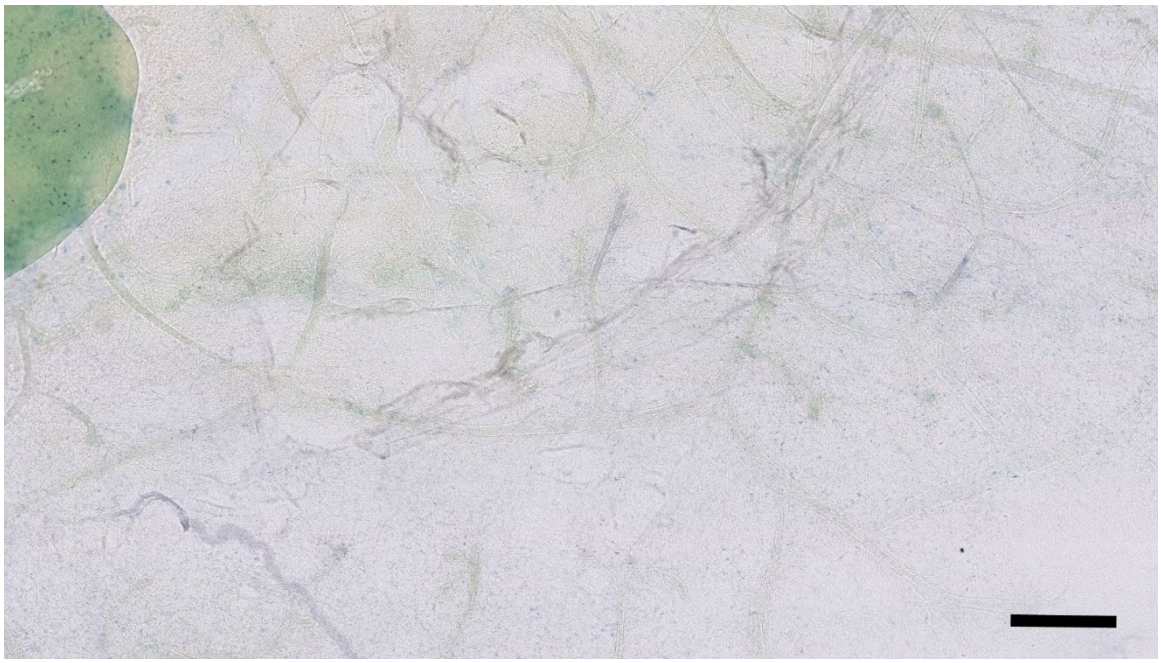

Supplementary Fig.3 Negative control of whole-mount mammary gland staining.

X-gal staining of a mammary gland from (*Cre*-, *LacZ*+) offspring from heterozygous Koi-4 was shown. The lymph node showed some blue signal, indicating that the lymph node could be stained nonspecifically. All the epithelium ducts did not show any blue signal, verifying the specificity of duct labeling of X-gal staining. Scale=500um

	track	ID	Cell/tissue	Organism	Restr. Enz.	Database	Database ID	Browser	Publication
Hi-C	1	Whole brain	whole brain	mm10	DNaseI	4DN	4DNFIQ48NYOW	WashU	Deng 2015
	https://4dn-open-data-public.s3.amazonaws.com/fourfront-webprod/wfoutput/60d98cc6-4583-4ebe-9c5a-77fc421ef560/4DNFIQ48NYOW.hic								
	2	NPC	NPC	mm10	DpnII	4DN	4DNFIHW8NTQX	WashU	Bonev 2017
	https://4dn-open-data-public.s3.amazonaws.com/fourfront-webprod/wfoutput/219497b5-3f35-473b-9d4e-e1cf21c69561/4DNFIHW8NTQX.hic								
	3	Cortex	cortex	mm10	MboI	4DN	4DNFII3JV8I1	WashU	Du 2017
	https://4dn-open-data-public.s3.amazonaws.com/fourfront-webprod/wfoutput/268b7d52-9655-474c-9467-8ba31bb2195c/4DNFII3JV8I1.hic								
	4	ESC	ESC	mm10	DpnII	4DN	4DNFIU8AF5ZY	WashU	Bonev 2017
	https://4dn-open-data-public.s3.amazonaws.com/fourfront-webprod/wfoutput/c2eaf9bf-9584-4cec-8685-bd74038a6c01/4DNFIU8AF5ZY.hic								
	5	Hepatocyte	hepatocyte	mm10	HindIII	4DN	4DNFIFULDMGN	WashU	Schwarzer 2017
	https://4dn-open-data-public.s3.amazonaws.com/fourfront-webprod/wfoutput/57ecaa79-5c9c-49c7-b841-0a4bf3117555/4DNFIFULDMGN.hic								
	6	Sperm	sperm	mm10	MboI	4DN	4DNFIN8F14CS	WashU	Du 2017
	https://4dn-open-data-public.s3.amazonaws.com/fourfront-webprod/wfoutput/27f54fcb-54fe-41a4-b25a-2f8944c89044/4DNFIN8F14CS.hic								

	Fig	Regions	Genes
WashU	A	chr6:104149809-119528368	Oxtr
	B	chr2:121804885-139358632	Oxt

Supplementary Table.1

The datasets IDs and sample information for mouse 3D chromatin verification

The database source of each mouse sample, analysis and visualization tool information, and the region analyzed was listed.